Peridynamic solutions to micropolar beam

Akash Gautam

A
Thesis submitted to
Indian Institute of Technology Hyderabad
In Partial Fulfillment of the Requirements for
The Degree of Master of Technology

भारतीय प्रौद्योगिकी संस्थान हैदराबाद
Indian Institute of Technology Hyderabad

DEPARTMENT OF CIVIL ENGINEERING

July 2019

Declaration

I declare that this written submission represents my ideas in my own words, and where others' ideas or words have been included, I have adequately cited and referenced the original sources. I also declare that I have adhered to all principles of academic honesty and integrity and have not misrepresented or fabricated or falsified any idea/data/fact/source in my submission. I understand that any violation of the above will be a cause for disciplinary action by the Institute and can also evoke penal action from the sources that have thus not been properly cited, or from whom proper permission has not been taken when needed.
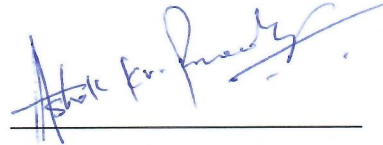
(Signature)
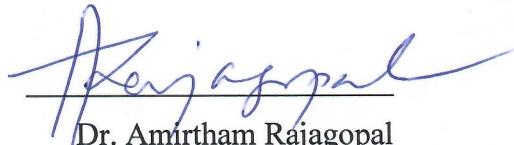
AKASH GAUTAM
CE17MTECH11017

ii

Approval Sheet

This thesis entitled Peridynamic Solutions for Beams by Akash Gautam is approved for the degree of Master of Technology from IIT Hyderabad.

Dr. Ashok Pandey

External Examiner

Dr. Mahendra Kumar Madhavan

Internal Examiner

Dr. Amirtham Rajagopal

Adviser

Dr. Ashok Pandey

Chairman

Acknowledgements

Firstly, I would like to express my sincere gratitude towards my adviser Dr. Amirtham Rajagopal for providing me this wonderful opportunity to work on peridynamics. Throughout the course of the thesis work, his interest in me and his exemplary guidance have always motivated me to think beyond conventional ways and explore new ideas.His motivated and ever positive personality encouraged me to believe in myself. I would like to thank Dr. Ashok Pandey, Associate Prof., Dept of Mechanical and Aerospace Eng, IITH and Dr.Mahendrakumar Madhavan, Associate Prof., Dept. of Civil Engg., IITH. I would like to express my gratitude towards Ms Preethi Kasirajan without whom I may not be able to complete my project. I would like to thank the faculties of Structural Eng, IITH - Dr. Amirtham Rajagopal,Prof. K.V.L. Subramaniam, Dr. Mahendrakumar Madhavan, Dr. Anil Agarwal, and Dr. Surendra Nadh Somala to help me understand the basics of my research during the course work . I would also like to thank Mr.Shiva Reddy, Mr. Surya Shekhar Reddy and Mr Aurojyoti Prusty, members of the Research group of my thesis advisor for their support. I would like to wholeheartedly thank Mr. Anvit Gadkar, Mr. Supraj Reddy, Mr.Rushikesh Bhangdiya, Mr. Ashutosh Nema, Mr. Amal Dev, Mr. Kishore Kumar and Mr. Sumit Sahoo for making my life wonderful at IITH.

Last but not the least I would also acknowledge the love and support provided by my parents, sister and well-wishers throughout this journey.

Abstract

Peridynamics (PD) is a non local continuum mechanics theory developed by Silling in 2000. The inception of peridynamics can be dated back to the works of Piola according to dell'Isola et al. [1]. Classical continuum theory (CCM) was there to study the materials response to deformation and loading conditions deformation response of materials and structures subjected to external loading conditions without taking into effect the atomistic structure. Classical continuum theory can be applied to various challenging problems but its governing equation have a limitation that it cannot be applied on any discontinuity such as a crack, as the partial derivatives with respect to space are not defined at a crack. To overcome this limitation , a new non local continuum approach i.e Peridynamics (PD) was developed.It was introduced as it governing equations donot contain any partial derivative with respect to space so it can be applied at cracks also. We can also think of Peridynamics as the continuum version of molecular dynamics. This behaviour of peridynamics makes it handy for multi-scale analysis of materials. Peridynamics finds it usefulness in other fields also such as moisture, thermal, fracture, aerospace etc., so that multiscale analysis can be done . The analysis of structure due to progressive failure is challenge. These challenges can be overcome by techniques such as using both nonlocal and classical (local) theories. But Peridynamic theory is computationally costly compared to the finite element method. While analyzing structures with compelxity , utilize structural idealizations is to be done to make computations feasible. Peridynamics has been catching the eyes of the researchers as its formulation include integral equations , unlike the partial differential equations in classical continuum theory. This method is still in early stages, a lot of research work is to be done to make it feasible for a large no. of problems.

Contents

List of Figures

3

Chapter 1

INTRODUCTION

Peridynamic is a non local continuum theory of solid mechanics based on integral equations originally proposed to address elasticity problems involving discontinuities. The governing equations of peridynamics are integro-differential equations and do not contain spatial derivatives which make this new theory very attractive for problems including discontinuities such as cracks.

1.1 Why going away from classical theory ?

In classical theory, a material point is influenced by the other material points which are in infinitesimally small neighbour, so it is a local theory which means stress at the material point depends only on the strain of material points in the infinitesimally small neighbour.For macroscale it can be true but not as the length scale approaches atomistic scale because of the involvement of longrange forces.Even for macroscale also, microstructure can have influence on the macrostructure.Even now there are no full proof theory to predict crack initiation and its path due to the mathematical formulation which assumes body as continous as the deformation occurs. So the formulations doesnot apply as soon as the discontinuity appears in the body.Classical theory involves partial differential equations with respect to space and these spatial derivatives are not defined at the discontinuities.So the main limitation of classical theory is that it is not applicable due to its governing equations which involve partial derivatives with respect to space when there is discontinuity such as a crack.

(a) Local (b) Peridynamics
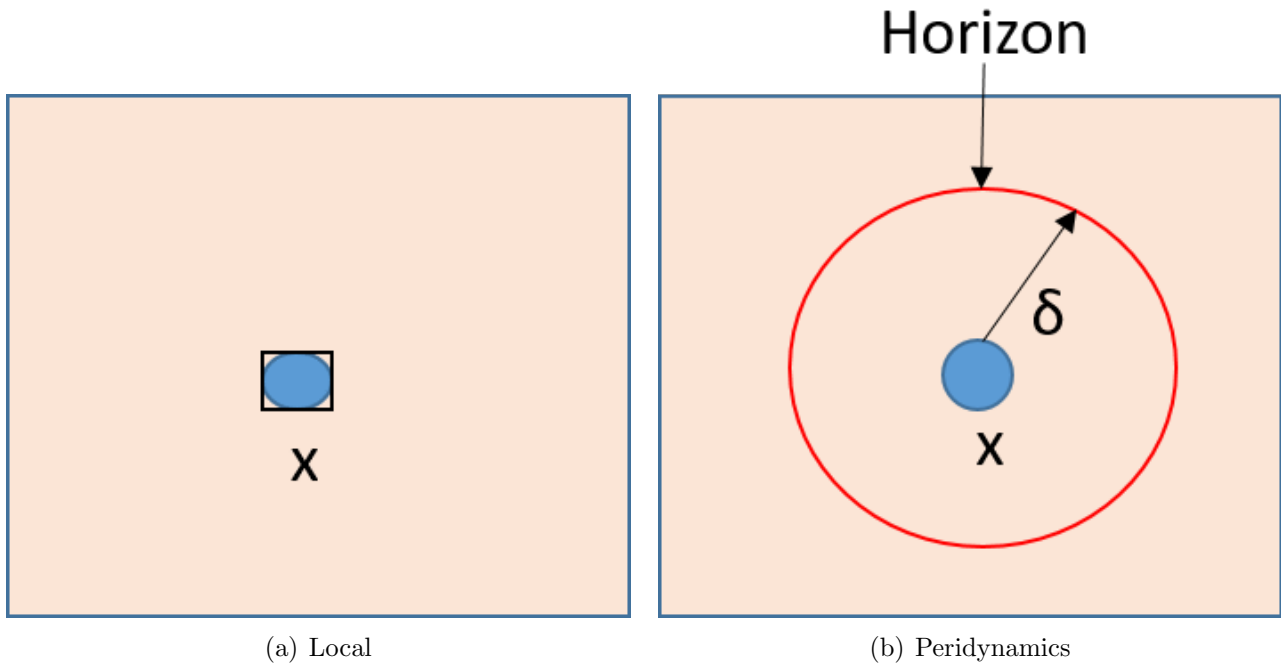
Figure 1.1: **Comparision between local and nonlocal theory**

The stress at crack tips tends to be infinite in classical theory which lead to the concept of Linear Elastic Fracture Mechanics (LEFM) which assumes pre-existing cracks in the material where crack initiation and crack path are treated separately using external parameters such as critical energy release rate. The critical energy release rate is not part of the governing equations of the classical theory. Further the calculation of energy release rate is challenging as the quantity depends on geometry, loading conditons and numerical methods.in addition to this separate criteria for crack propagation is needed.

The classical theory solutions are independent of crack size but the experiments showed that materials with small cracks have more fracture resistance. Also classical theory predicts there is no dispersion which is not true as the experiments shows otherwise for the propagation of elastic plane waves with shorter wavelengths in elastic solids. Hence no internal length parameter is there to distinguish different length scales.
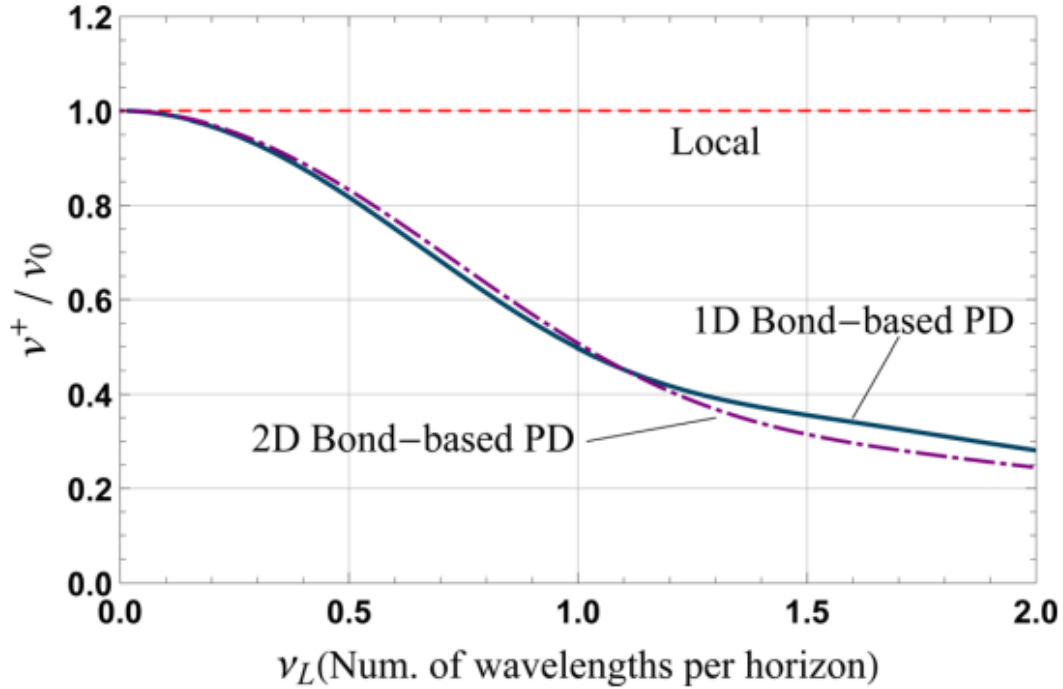
Figure 1.2: **Comparison of phase velocity for wave propagation**

However classical theory is not capable to distinguish different length scales but it can capture failure processes by using Finite Element Method (FEM).In fracture mechanics main worry is the introduction of pre-existing cracks not the new cracks.When addressing the pre-existing crack growth , FEM using traditional elements have the limitation of remeshing after each incremental growth of a crack.

Hence the presence of infinite stress at crack tip, need for external parameters, inability to distinguish crack size and crack initiation, and requirement for remeshing makes impossible to solve probems with multiple interacting cracks propagating in unusual manner using traditional FEM elements.

1.2 Basic Definitions

1.2.1 Equation of Motion

The peridynamic equation of motion of any particle X in reference configuration at time t is given as

$$\rho \frac{\partial^2 u}{\partial t^2} = \int_R f\left(u(\boldsymbol{X}',t) - u(\boldsymbol{X},t), \boldsymbol{X}' - \boldsymbol{X}\right) dV_{\boldsymbol{X}'} + b\left(\boldsymbol{X},t\right) \tag{1.1}$$

where $V_{\boldsymbol{X}'}$ is a neighborhood of X , u is the displacement vector field, b is prescribed body force density field, ρ is the mass density in reference configuration and $\boldsymbol{f}$ is a pairwise force function whose value is the force vector (per unit volume squared) that the particle X' exerts on particle X.
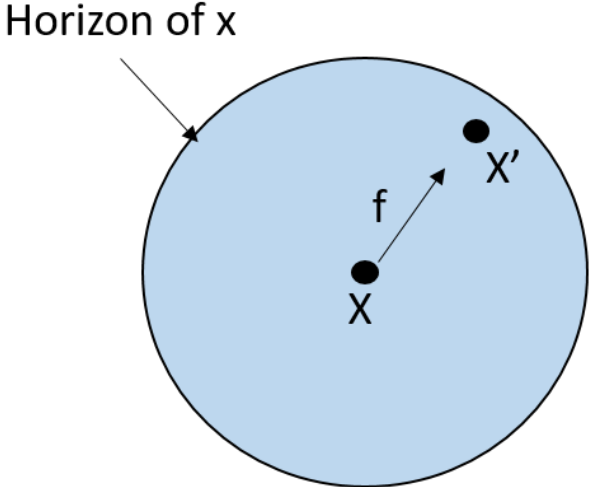
Figure 1.3: **Particle interaction in a horizon**

1.2.2 Relative Position

The relative position of the two particles in the reference state is ξ which is equal to

$$\xi = \boldsymbol{X}' - \boldsymbol{X} \tag{1.2}$$

1.2.3 Relative Displacement

The relative displacement of the two particles is $\boldsymbol{\eta}$ which is equal to

$$\boldsymbol{\eta} = \boldsymbol{u}\left(\boldsymbol{X'}, t\right) - \boldsymbol{u}\left(\boldsymbol{X}, t\right) \tag{1.3}$$
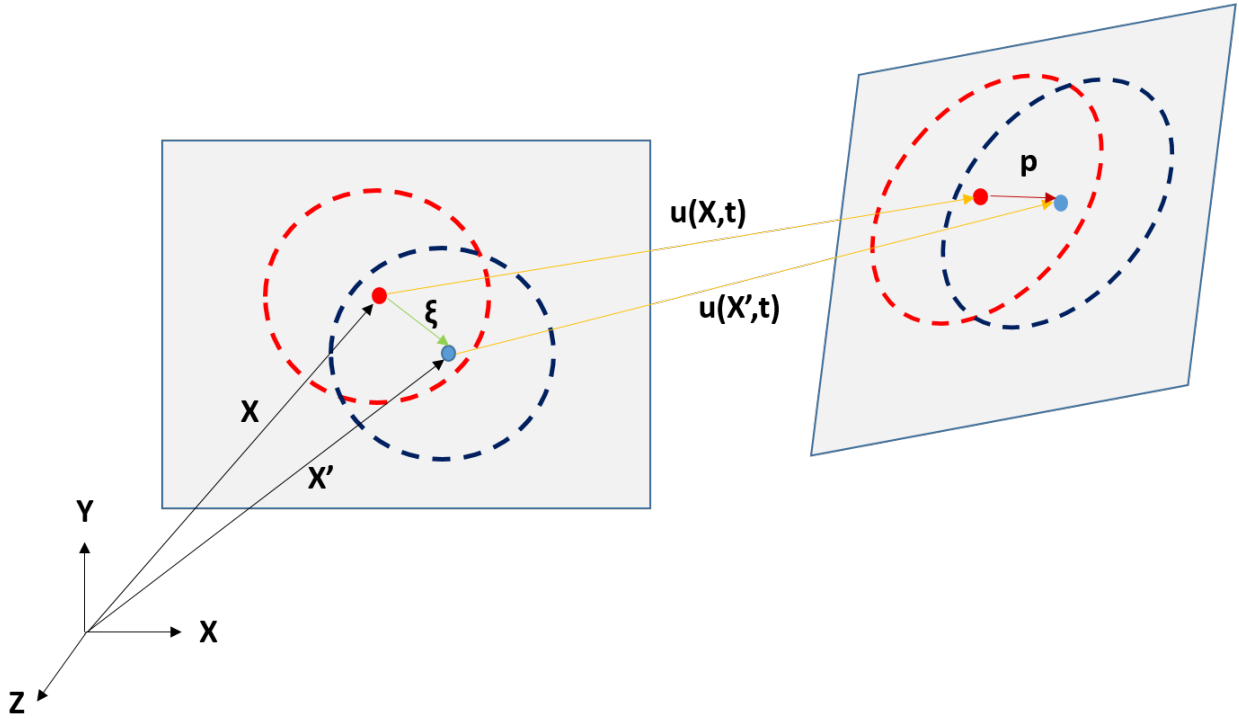
Figure 1.4: **Particle interaction in a horizon**

The relative position of the particles in the deformed state p which is equal to $\boldsymbol{\eta} + \xi$.

1.2.4 Conservation laws

The linear and angular momentum law is to be followed by the force function f that is

$$\boldsymbol{f}\left(-\boldsymbol{\eta}, -\xi\right) = -\boldsymbol{f}\left(\boldsymbol{\eta}, \xi\right) \tag{1.4}$$

$$\left(\boldsymbol{\eta} + \xi\right) * \boldsymbol{f}\left(\boldsymbol{\eta}, \xi\right) = 0 \tag{1.5}$$

for all $\xi, \boldsymbol{\eta}$. The above expressions implies that the relative position is parallel to the force between the two particles. The general form of the bond force for the basic theory can be written as

$$\boldsymbol{f}(\boldsymbol{\eta}, \xi) = \frac{\xi + \boldsymbol{\eta}}{|\xi + \boldsymbol{\eta}|} f(\boldsymbol{p}, \xi, t) \tag{1.6}$$

where the scalar bond force is represented as f and also

$$\boldsymbol{p} = |\boldsymbol{\eta} + \xi|. \tag{1.7}$$

1.2.5   Bond stretch

Like in classical theory , where there is a strain, here it is a scalar bond stretch $'s_b'$ which is defined as

$$s_b = \frac{|\xi + \boldsymbol{\eta}| - |\boldsymbol{\eta}|}{|\xi|} \tag{1.8}$$

For a brittle material to be microelastic, it should have

$$f(s, t, \xi) = \chi(t, \xi) c s_b \tag{1.9}$$

where χ is a history dependent damage function taking values of either 0 or 1 and c representing spring constant

$$\chi(t, \xi) = 1 \text{ if } s_b(t', \xi) < s_o \text{ for all } 0 \le t' \le t \tag{1.10}$$
$$= 0 \text{ otherwise} \tag{1.11}$$

where s_o is the critical bond stretch for failure which means if the bond stretch is has exceeding critical bond stretch, the bond is assumed broken. The value of spring constant c is found by equating the energy density within the horizon in the peridynamic theory to strain energy under isotropic extension from continuum mechanics for the same deformation. Thus

$$c = \frac{18K}{\pi \delta^4} \tag{1.12}$$

where δ is the horizon. The critical stretch for bond failure , s_o is related to the energy release rate G as

$$s_o = \left(\frac{10G}{\pi c \delta^5}\right)^{\frac{1}{2}} = \left(\frac{5G}{9K\delta}\right)^{\frac{1}{2}} \tag{1.13}$$

This is obtained by equating work done to break all bonds in a unit area to energy release rate Silling and Askari (2005) described that introduction of failure at interaction level leads to local damage at a point given by

$$\frac{1 - \int_V \chi\left(\boldsymbol{X}, t, \xi\right) dV_{\boldsymbol{X}}}{\int_V dV_{\boldsymbol{X}}} \tag{1.14}$$

where R represents spherical volume with radius equal to horizon of δ and the centre of sphere is at $\boldsymbol{X}$. So we can get the definition of the local damage at a point as ratio of amount of broken interactions to total amount of interactions .

1.3   Horizon size

Horizon of a material point refers to the region in which it has its influence on the other material points i.e it can have interactions with other material points in that region only. It is a length-scale parameter from which peridynamics gets its non-local behaviour.The type of the problem and its nature defines the selection of the horizon size. If the problem is not having any non-local behaviour,horizon should converge to zero In which case, classical continuum theory and peridynamics are equivalent of each other.We use the numerical techniques to solve the problems in peridynamics.Using a very small value of horizon size , the computational time gets very large. So that size of horizon should be chosen which doesn't show any significant non-local character which we can get by doing some convergence study. In problems which have non-local and non-classical behaviour horizon is used as a length scale parameter which we can adjust according to the required physical behaviour that can be correctly represented.In a beam where crack is to appear or loading is applied , we cannot choose uniform size of horizon all over the beam, the region in which it is assumed for the crack to appear and the loading, we can have a smaller horizon of each material point.For the problems in which the cross section area of the material is changing, we can use small horizon size to accurately detect the behaviour of material at the change of cross section.

1.4   Advantages and Limitations

- Advantages

    - Offers potentially great generality in fracture modeling.
        * Cracks nucleate and grow spontaneously.
        * Cracks follow from the basic field equations.

- Any material model from local theory can be used.
- Compatible with molecular scale long-range forces.
- Length scale can be exploited for multiscale modeling.

- Limitations

  - Slow due to many interactions.
  - Need smarter integration methods.
  - surface effects: correction methods are available but none totally satisfactory.
  - boundary conditions are different from the local theory.
  - Particle discretization has known limitations.

Chapter 2

LITERATURE REVIEW

The nonlocal peridynamic theory has been proven to be a promising method for modelling the material failure and damage analysis in solid mechanics .The modelling of complex fracture problems such as crack branching and spontaneous crack nucleation and , curving and arrest can be done easily using the integro differential equations of peridynamics. Ning et al. [2] studied the damage due to impact in a three point bending beam with offset notch using the peridynamic approach which is widely used for the mixed I-II crack propagation in brittle materials . The predictions from the peridynamic analysis agree well with available experimental observations. The numerical results show that the dynamic fracture behaviour of the beam under the impact load such as crack initiation, curving and branching rely on the location of offset notch and the impact speed of the drop hammer. It has been observed that in modal response of an aluminium plate with clamped free boundary conditions, the natural frequencies from peridynamics agree better with the experimental results than the frequencies from finite elements for all modes except mode I [3]. Differences between peridynamics and experiment results ranged (in magnitude)from 0.13 to 10.38% and between pridynamic and finite-elements from 0.23% to 9.72%. The non local peridynamic theory is applied to study the structural vibration and impact damage using 2D bond based peridynamics and the the numerical results indicate that the peridynamic solutions for beams vibration problems are almost identical to the results based on Euler-Bernoulli beam theory. It is also found that the feature of softer material near the boundary in peridynamics has a notable effect on the solution of beam vibration [4]. Gardy et al. [5] developed a new state based peridynamic model which is used to represent the bending of an Euler-Bernoulli beam. This model is found to give accurate deformation results for simple beam tests. The perfect plasticity and simple brittle damage models successfully reproduce the impact of non-linear behaviours on deformation of rectangular cantilever and the framework is laid to allow application of the same models to I-beams. This novel model simplifies treatment of bending in beams and

is extensible to bending in plates. Silling et al. [6] used PD theory for damage prediction considering Kalthoff-Winkler experiment [7], in which a plate having two parallel notches is hit by impactor and peridynamic simulations successfully captured angle of crack growth that is observed in the experiments. This technique does not reqiure the specification of kinetic laws for crack growth and because it does not require the tracking of individual cracks, it models fracture mechanics problems of arbitrary complexity with potentially great generality. Silling and Askari [8] showed the convergence of peridynamics using a plate with a centre crack. Gardy et al. [9], using the peridynamic state based beam model, determined the bending of a Kirchoff-Love plate. This model is non ordinary and is derived from the concept of a rotational spring between bonds. This simple extension of beam model reproduces plate bending with a poisson ratio of 0.33, which can be combined with a 2D linear peridynamic solid model to simulate mixed in-plane and transverse loading. Peridynamic theory can be applied to fracture problems in contrast to the approach of fracture mechanics. By using peridynamics, the crack path for inclined crack under dynamic loading were investigated. The peridynamics solution for this problem represents the main features of dynamic crack propagation such as crack bifurcation. The problem is solved for various angles and different stress values. The results are compared with molecular dynamic solutions that seem to show reasonable agreement in branching position and time [10]. High velocity impact and shock or blast responses are a critical design characteristic determing sizing of composite parts and ultimately weight savings .Peridynamis can be used to accurately predict nonlinear transient deformations and damage behaviour of compositess under shock or blast type of loadings due to explosions .Peridynamics provide the ability to predict residual strength and durability for improving structural designs of composites under such loadings[11]. Yile et al. [12] studied the delamination and the effect of fiber waviness using PD. It is shown that the simulations correctly perdicted the damage initiation and progression in the double cantilever beam (DCB) made up of laminated composite with wavy fibers. Jifeng et al. [13] et al. studied delmination and matrix damage process in composite laminates due to low velocity impact, and the simulations showed that damage area correlates very well with the experimental data. The peridynamic formulation for a unidirectional fiber-reinforced composite lamina based on homogenization and mapping between elastic and fracture parameters of the micro-scale peridynamic bonds and the macro-scale parameters of the composite is developed by Wenke et al. [14]. The model is then used to analyze the splitting mode (mode II) fracture in dynamic loading of a 0° lamina. Appropriate scaling factors are used in the model in order to have the elastic strain energy, for a fixed nonlocal interaction distance (the peridynamic horizon). Yozo et al. [15] developed a systematic analytical treatment of peristatic and peridynamic problems for a 1D infinite rod. It is found from the study that some peridynamic materials can have negative group velocities in certain regions of wavenumber. This indicates that peridynamics can also be used for modeling certain types

of dispersive media with anomalous dispersion. Sarego et al.[16] developed a 2D linearized ordinary state-based peridynamic model. The convergence behavior of peridynamic solutions in terms of the size of the nonlocal region by comparison with the classical (local) mechanics model is also studied. The degree to which the peridynamic surface effect influences the recovery of elastic properties is examined, and stress/strain recovery values are found to have a definite influence on the results. The technique used here can provide the basis for applying 2D peridynamic models to the study of fatigue failure and quasi-static fracture problems. The PD model developed by Le et al. [17] for plane stress and plane strain was studied and validated using a two dimensional rectangular plate with a round hole in the middle under constant tensile stress. The model is found to show the m -convergence and δ - convergence behaviors. The problem of cracks propagation in thin orthotropic flat plates under bending loads was studied by Tastan et al. [18] using peridynamics. The formulation followed here is based on the main ideas of bond based Peridynamics. Several numerical examples show that the results obtained with the new approach are in good agreement with those obtained with more classical computational methods. Moreover the numerically computed crack patterns seem to follow in a reasonable way the orthotropic properties of the models . Michael et al.[19] developed a plate model as a two-dimensional approximation of the three-dimensional bond-based theory of peridynamics via an asymptotic analysis. The resulting plate theory is demonstrated using a specially designed peridynamics code to simulate the fracture of a brittle plate with a central crack under tensile loading.

Chapter 3

APPLICATION TO EULER BERNOULLI BEAM

Every object in the world has a 3-Dimensional geometrical shape and it is usually possible to model structures in a 3-Dimensional fashion although this approach can be computationally expensive. In order to reduce computational time, the 3-Dimensional geometry can be simplified as a beam, plate or shell type of structure depending on the geometry and loading. This simplification should also be accurately reflected in the formulation which is used for the analysis. In this study, we want to develop Euler-Bernoulli beam formulation within ordinary-state based peridynamic framework. The equation of motion can be obtained by utilizing Euler-Lagrange equations. The accuracy of the formulation is validated by considering various benchmark problems subjected to different loading and displacement/rotation boundary conditions.

3.1   Formulation

To represent an Euler Bernoulli Beam, we descretize the beam into single row of material points. The descretization is meshless and the shape of the horizon is a line . Each material point is having only one degree of freedom that is transverse displacement along z-axis.

Consider two material points k and j with coordinates x_k and x_j and their transverse displacements as u_k and u_j, with volume of horizon around each material point as V_k and V_j respectively.After deformation, let κ_k andκ_j are their curvatures.
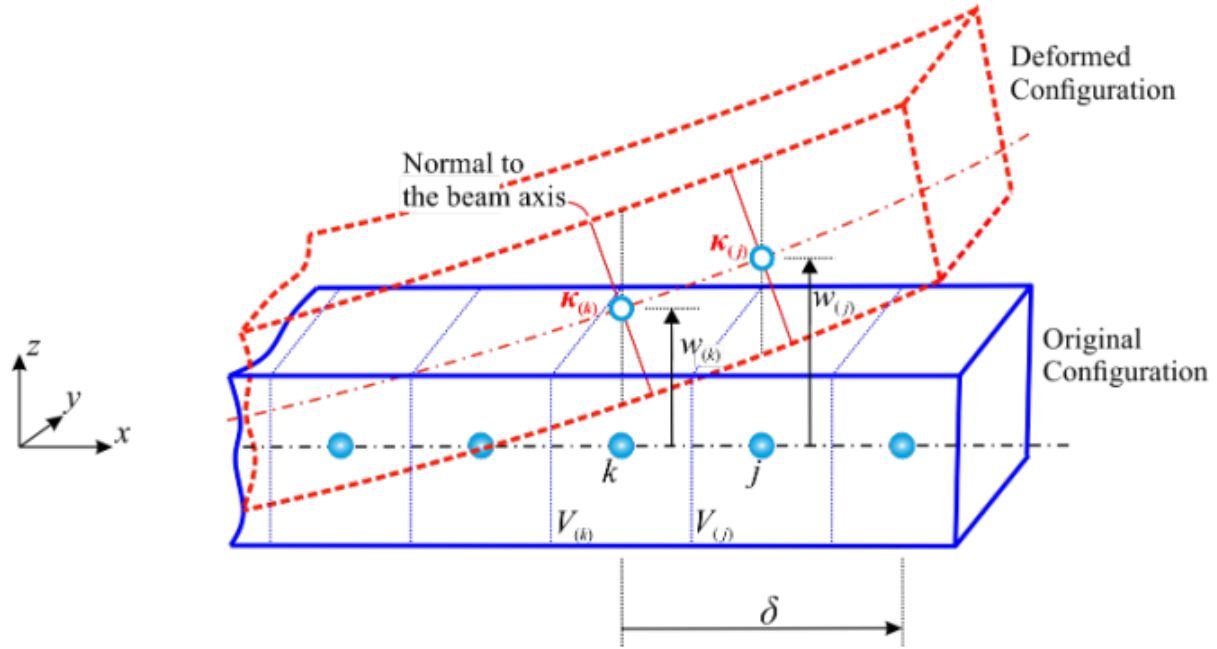
Figure 3.1: **Kinematics of Euler Bernoulli Beam**

$x_k \rightarrow$material point coordinate
$V_k \rightarrow$incremental volume
$\rho \rightarrow$mass density
$u_k \rightarrow$displacement

3.1.1 Equation of Motion

The strain energy density function in terms of micro-potentials for material point k is

$$W_k = \frac{1}{2} \sum_{j=1}^{\infty} \frac{1}{2}(\alpha_{kj} + \alpha_{jk})V_j \tag{3.1}$$

where the micropotential can be defined as the energy required to break the bond between two material points per unit volume square.

The micropotentials are also the functions of the transverse degree of freedom of the material points.

The PD equation of motion at material point x_k is found out using principal of virtual work which is

$$\delta \int_{t_o}^{t_1} (T - U)dt = 0 \tag{3.2}$$

where T and U are the total kinetic and total potential energies of the system
Total kinetic energy of the system is due to bending and transverse shear deformation total potential energy is obtained by the summation of micropotentials

$$T = \frac{1}{2} \sum_{j=1}^{\infty} \rho_i \dot{u}_i \cdot \dot{u}_i V_i \tag{3.3}$$

$$U = \sum_{i=1}^{\infty} W_i V_i - \sum_{i=1}^{\infty} (b_i \cdot \dot{u}_i) V_i \tag{3.4}$$

Using equation (3.1)

$$U = \sum_{i=1}^{\infty} \left(\frac{1}{2} \sum_{j=1}^{\infty} \frac{1}{2} (\alpha_{ij} + \alpha_{ji}) V_j) V_i \right) - \sum_{i=1}^{\infty} (b_i \cdot \dot{u}_i) V_i \tag{3.5}$$

Lagrangian $L = T - U$

$$L = \cdots \frac{1}{2} \rho_k \dot{u}_k \cdot \dot{u}_k V_k \cdots$$
$$\cdots - \frac{1}{2} \sum_{j=1}^{\infty} \{ \frac{1}{2} [\alpha_{kj}(u_{1^k} - u_k, u_{2^k} - u_k, \cdots)$$
$$+ \alpha_{jk}(u_{1^j} - u_j, u_{2^j} - u^j, \cdots)] V_j \} V_k \cdots \tag{3.6}$$
$$\cdots - \frac{1}{2} \sum_{i=1}^{\infty} \{ \frac{1}{2} [\alpha_{ik}(u_{1^i} - u_i, u_{2^i} - u_i, \cdots)$$
$$+ \alpha_{ki}(u_{1^k} - u_k, u_{2^k} - u^k, \cdots)] V_i \} V_k \cdots$$
$$+ (b_k \cdot \dot{u}_k) V_k \cdots$$

or

$$L = \cdots \frac{1}{2}\rho_k \dot{u}_k \cdot \dot{u}_k V_k \cdots$$

$$\cdots - \frac{1}{2}\sum_{j=1}^{\infty}\{\alpha_{kj}(u_{1^k} - u_k, u_{2^k} - u_k, \cdots)V_j V_k\}\cdots$$

$$\cdots - \frac{1}{2}\sum_{j=1}^{\infty}\{\alpha_{jk}(u_{1^j} - u_j, u_{2^j} - u_j, \cdots)V_j V_k\}\cdots \qquad (3.7)$$

$$\cdots + (b_k \cdot \dot{u}_k)V_k \cdots$$

Here u_{1_j}, u_{2_j},.. are the neighbourhood material points of j within the horizon. Similarly u_{1_k}, u_{2_k},.. are the neighbourhood material points of k within the horizon. Putting the value of lagrangian L from equation (3.7) in lagrangian equation

$$\frac{\partial}{\partial t}\left(\frac{\partial}{\partial \dot{u}_k}\right) - \frac{\partial L}{\partial u_k} = 0$$

$$(3.8)$$

$$\rho_k \ddot{u}_k V_k + \left(\sum_{j=1}^{\infty}\frac{1}{2}\left(\sum_{i=1}^{\infty}\frac{\partial \alpha_{ij}}{\partial(u_j - u_i)}V_i\right)\frac{\partial(u_j - u_i)}{u_k} + \sum_{j=1}^{\infty}\frac{1}{2}\left(\sum_{i=1}^{\infty}\frac{\partial \alpha_{ik}}{\partial(u_k - u_i)}V_i\right)\frac{\partial(u_k - u_i)}{u_k} - b_k\right)V_k = 0$$

or

$$\rho_k \ddot{u}_k = \sum_{j=1}^{\infty}\frac{1}{2}\left(\sum_{i=1}^{\infty}\frac{\partial \alpha_{ki}}{\partial(u_i - u_k)}V_i\right) - \sum_{j=1}^{\infty}\frac{1}{2}\left(\sum_{i=1}^{\infty}\frac{\partial \alpha_{ik}}{\partial(u_k - u_i)}V_i\right) + b_k \qquad (3.9)$$

Using dimensional analysis, we come to know that the term $\sum_{i=1}^{\infty}\frac{\partial \alpha_{ki}}{\partial(u_j - u_k)}V_i$ represents the force term.

Let this term be the force density the material point x_j exerts on x_k. So the equation (3.9) can be written as

$$\rho_k \ddot{u}_k = \sum_{j=1}^{\infty}(\tilde{t}_{kj} - \tilde{t}_{jk})V_j + \hat{b}_k \qquad (3.10)$$

19

where the tilde sign shows the force densities due to bending deformations

$$\tilde{t}_{kj} = \frac{1}{2V_j} \sum_{i=1}^{\infty} \frac{\partial \alpha_{ki}}{\partial(u_j - u_k)} V_i = \frac{1}{V_j} \frac{\partial \left(\frac{1}{2} \sum_{i=1}^{\infty} \alpha_{ki} V_i \right)}{\partial(u_j - u_k)} V_i \tag{3.11}$$

$$= \frac{1}{V_j} \frac{\partial W_k}{\partial(u_j - u_k)} \tag{3.12}$$

Using classical continuum mechanics, the strain energy density for material points k can be represented as

$$W_k = \frac{1}{2} a \kappa_k^2 \tag{3.13}$$

where κ_k is curvature of material point k and a is peridynamic constant
The curvature for material point k can be defined as

$$\kappa_k = d \sum_{i^k}^{\infty} \frac{u_{i^k} - u_k}{\xi_{i^k k}^2} V_{i^k} \tag{3.14}$$

where i^k represents all material points inside the horizon of material point k and d is also a peridynamic constant

$$\xi_{i^k k} = |x_k - x_{i^k}| \tag{3.15}$$

Putting the value of κ_k in eq.(3.13),we get

$$W_k = \frac{1}{2} a d^2 \left(\sum_{i^k}^{\infty} \frac{u_{i^k} - u_k}{\xi_{i^k k}^2} V_{i^k} \right)^2 \tag{3.16}$$

Putting value of W_k in equation (3.12) we get

$$\tilde{t}_{kj} = \frac{a d^2}{V_{i^k}} \left(\sum_{i^k}^{\infty} \frac{u_{i^k} - u_k}{\xi_{i^k k}^2} V_{i^k} \right) \frac{V_{i^k}}{\xi_{i^k k}^2} = \frac{a d \kappa_k}{\xi_{jk}^2} \tag{3.17}$$

Simlarly the value of $\tilde{t}_{jk}$ is found and those values are put in eq. 3.10 to get equation of motion as

$$\rho_k \ddot{u}_k = ad^2 \sum_{j=1}^{\infty} \frac{1}{\xi_{jk}^2} \left(\sum_{i^k=1}^{\infty} \frac{u_{i^k} - u_k}{\xi_{i^k k}^2} V_{i^k} - \sum_{i^j=1}^{\infty} \frac{u_{i^j} - u_j}{\xi_{i^j j}^2} V_{i^j} \right) V_j + \hat{b}_k \qquad (3.18)$$

3.1.2   Validation with classical theory

The validity of the equation is to be checked and to check so we limit the horizon nsize to zero to get classical continuum theory i.e $\delta \to 0$
Using Taylor series expansion the transverse displacements is expressed in terms of their main material point displacements and ignoring higher order terms

$$u_{i^k} = u_k + \xi_{i^k k} u_{k,x} sgn(x_{i^k k} - x_k) + \frac{\xi_{i^k k}^2}{2} u_{k,xx} \qquad (3.19)$$

Putting value from eq. (3.19) in eq. (3.18), we get

$$\rho_k \ddot{u}_k = ad^2 \sum_{j=1}^{\infty} \frac{1}{\xi_{jk}^2} \left(\sum_{i^k=1}^{\infty} \frac{-\xi_{i^k k} u_{k,x} + \frac{\xi_{i^k k}^2}{2} u_{k,xx}}{\xi_{i^k k}^2} V_{i^k} - \sum_{i^j=1}^{\infty} \frac{\xi_{i^j j} u_{j,x} + \frac{\xi_{i^j j}^2}{2} u_{j,xx}}{\xi_{i^j j}^2} V_{i^j} \right) V_j + \hat{b}_k$$

$$(3.20)$$

$$\rho_k \ddot{u}_k = ad^2 \sum_{j=1}^{\infty} \frac{1}{\xi_{jk}^2} \left(\sum_{i^k=1}^{-\infty} \frac{u_{k,xx}}{2} V_{i^k} + \sum_{i^k=1}^{\infty} \frac{u_{k,xx}}{2} V_{i^k} - \sum_{i^j=1}^{-\infty} \frac{u_{j,xx}}{2} V_{i^j} - \sum_{i^j=1}^{\infty} \frac{u_{k,xx}}{2} V_{i^j} \right) V_j + \hat{b}_k$$

$$(3.21)$$

The summation sign includes all the material points in the horizon of main material point on the left and right of the material point.
If similar expansion is done for material point j we have

$$u_{j,xx} = u_{k,xx} + \xi_{jk} u_{k,xxx} sgn(x_j - x_k) + \frac{\xi_{jk}^2}{2} u_{k,xxxx} \qquad (3.22)$$

21

Putting value from eq. (3.22) to eq. (3.21)

$$\rho_k \ddot{u}_k = ad^2 \sum_{j=1}^{-\infty} \frac{1}{\xi_{jk}^2} \left(\sum_{i^j=1}^{-\infty} \frac{\xi_{jk} u_{k,xxx} - \frac{\xi_{jk}^2}{2} u_{k,xxxx}}{2} V_{i^j} + \sum_{i^j=1}^{\infty} \frac{\xi_{jk} u_{k,xxx} - \frac{\xi_{jk}^2}{2} u_{k,xxxx}}{2} V_{i^j} \right) V_j$$

$$+ad^2 \sum_{j=1}^{\infty} \frac{1}{\xi_{jk}^2} \left(\sum_{i^j=1}^{-\infty} \frac{-\xi_{jk} u_{k,xxx} - \frac{\xi_{jk}^2}{2} u_{k,xxxx}}{2} V_{i^j} + \sum_{i^j=1}^{\infty} \frac{-\xi_{jk} u_{k,xxx} - \frac{\xi_{jk}^2}{2} u_{k,xxxx}}{2} V_{i^j} \right) V_j + \hat{b}_k$$

$$(3.23)$$

Doing some algebraic calculations,we have the final equation of motion for peridynamics as

$$\rho_k \ddot{u}_k = -ad^2 \sum_{j=1}^{\infty} \left(\sum_{i=1}^{\infty} \frac{u_{k,xxxx}}{4} V_i \right) V_j + \hat{b}_k \tag{3.24}$$

where i^j is replaced by i
The infinitesimal volumes V_i and V_j can be expressed as

$$V_i = A \Delta \xi_{ik} \tag{3.25}$$
$$V_j = A \Delta \xi_{jk} \tag{3.26}$$

$\Delta \xi_{ik}$ tends to $d\xi^{"}$ and $\Delta \xi_{jk}$ tends to $\rightarrow d\xi'$
Converting summations of eq.(3.24) into integrals, we have

$$\rho \ddot{u} = -ad^2 A^2 \int_{-\delta}^{\delta} \int_{-\delta}^{\delta} \frac{u_{,xxxx}}{4} d\xi^{"} d\xi' + \hat{b} \tag{3.27}$$

$$\rho \ddot{u} + A^2 ad^2 \delta^2 \frac{\partial^4 u}{\partial x^4} = \hat{b} \tag{3.28}$$

Also in classical continuum mechanics the EOM for Euler Bernoulli beam is

$$\rho \ddot{u} + \frac{EI}{A} \frac{\partial^4 u}{\partial x^4} = p - \frac{\partial m}{\partial x} \tag{3.29}$$

22

where p is the transverse load and $\dfrac{\partial m}{\partial x}$ is the change in acting on a material volume.
Comparing eq. (3.28) and eq. (3.29) we get

$$a = \frac{EI}{A^3 d^2 \delta^2} \tag{3.30}$$

$$b = p - \frac{\partial m}{\partial x} \tag{3.31}$$

We can calculate peridynamic material parameter d, by comparing the curvature of material point in peridynamics with curvature in classical theory under a simple loading condition with constant curvature υ i.e

$$k = \upsilon = \frac{\partial^2 u}{\partial x^2} \tag{3.32}$$

Integrating above equation, we get

$$u_x = \frac{\upsilon x^2}{2} + ax + b \tag{3.33}$$

At $x = \delta$ and $x = -\delta$, y=0.Satisfying these conditions we have

$$u = \frac{\upsilon x^2}{2} - \frac{\upsilon \delta^2}{2} \tag{3.34}$$

At x=0, $u_k = -\frac{\upsilon \delta^2}{2}$
At $x = \xi$, $u_{ik} = \frac{\upsilon \xi^2}{2} - \frac{\upsilon \delta^2}{2}$
Putting the value of u_{ik} and u_k in eq. 3.14 we get

$$\kappa_k = d \sum_{i^k=1}^{\infty} \frac{\upsilon}{2} V_{ik} \tag{3.35}$$

$$\kappa_k = d\frac{\upsilon}{2} \int_{-\delta}^{\delta} A d\xi^{"} \tag{3.36}$$

$$\kappa_k = d\upsilon A\delta \tag{3.37}$$

Equating above value with υ we get

$$d = \frac{1}{A\delta} \tag{3.38}$$

Putting the value of d in eq. (3.30)

$$a = \frac{EIA^2\delta^2}{A^3\delta^2} \tag{3.39}$$

$$a = \frac{EI}{A} \tag{3.40}$$

Putting the value of a in (3.13) we get

$$W_k = \frac{1}{2}\frac{EI}{A}\kappa_k^2 \tag{3.41}$$

which is same as the strain energy density function in the classical theory.

This shows that we can recover classical theory by reducing horizon size in peridynamics to zero.

Chapter 4

APPLICATION TO TIMOSHENKO BEAM

Progressive failure analysis of structures is still a major challenge. There exist various predictive techniques to tackle this challenge by using both classical (local) and nonlocal theories. Peridynamic (PD) theory (nonlocal) is very suitable for this challenge, but computationally costly with respect to the finite element method. When analyzing complex structures, it is necessary to utilize structural idealizations to make the computations feasible. Therefore, this study presents the PD equations of motions for structural idealizations such as beams while accounting for transverse shear deformation. Also, their PD dispersion relations are to be presented and compared with those of classical theory .

4.1 Formulation

For a Timoshenko Beam also, we descretize the beam into single row of material points. The descretization is meshless and the shape of the horizon is a line . Each material point is having only one degree of freedom that is transverse displacement along z-axis.But alongwith the transverse displacement we have the shear deformation also.

Consider two material points k and j with coordinates x_k and x_j and their transverse displacements as u_k and u_j, shear deformation as φ_k and φ_j, out of plane rotations as θ_k and θ_j with volume of horizon around each material point as V_k and V_j respectively.After deformation, let κ_k and κ_j are their curvatures.
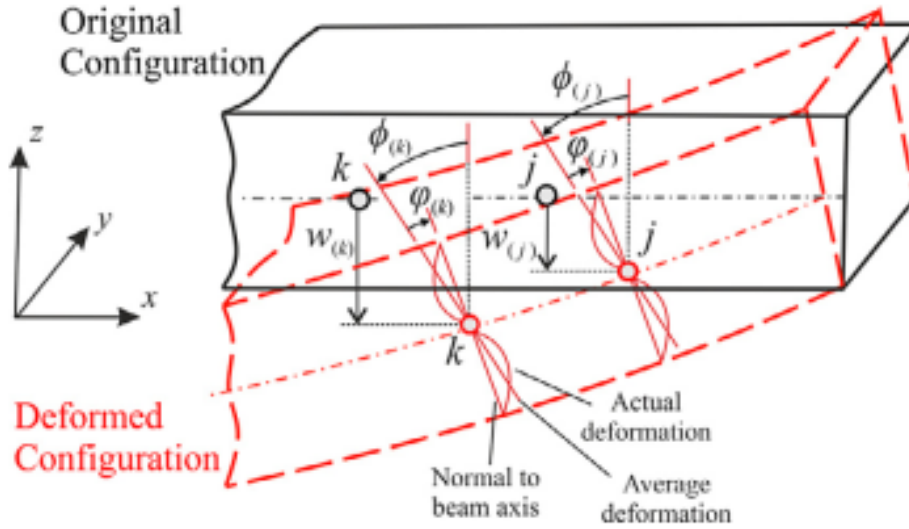
Figure 4.1: **Kinematics of Timoshenko Beam**

ϑ_k, ϑ_j are transverse shear angles
u_k, u_j are out of plane deflections
θ_k, θ_j are out of plane rotations

$$\vartheta_j = \frac{u_j - u_k}{\xi_{jk}} - \theta_j sign\left(x_j - x_k\right) \tag{4.1}$$

$$\vartheta_k = \frac{u_j - u_k}{\xi_{jk}} - \theta_k sign\left(x_j - x_k\right) \tag{4.2}$$

Assuming ϑ_{kj} as the average tansverse shear deformation due to the interaction between material points j and k

$$\vartheta_{kj} = \frac{u_j - u_k}{\xi_{jk}} - \frac{\theta_j + \theta_k}{2} sign(x_j - x_k) \tag{4.3}$$

Let κ_{kj} is curvature between material points j and k

$$\kappa_{kj} = \frac{\theta_j - \theta_k}{\xi_{jk}} \tag{4.4}$$

Similarly for material point j

$$\vartheta_{jk} = \frac{u_k - u_j}{\xi_{jk}} - \left(-\frac{\theta_j + \theta_k}{2}\right) sign(x_j - x_k) \tag{4.5}$$

$$\vartheta_{jk} = -\vartheta_{kj} \tag{4.6}$$

$$\kappa_{kj} = \frac{\theta_k - \theta_j}{\xi_{jk}} = -\kappa_{jk} \tag{4.7}$$

4.1.1   Equations of Motion

The PD equation of motion at material point x_k is found out using principal of virtual work which is

$$\delta \int_0^{t_1} (T - U)dt = 0 \tag{4.8}$$

where T and U are the total kinetic and total potential energies of the system

Total kinetic energy of the system is due to bending and transverse shear deformation total potential energy is obtained by the summation of micropotentials
Let $\tilde{\alpha}_{kj}(\kappa_{kj})$ and $\hat{\alpha}_{kj}(\vartheta_{kj})$ are micropotentials between material points arising from bending and transverse shear deformation respectively.

$$T = \frac{1}{2} \sum_{k=1}^{\infty} \rho \left[\dot{u_k}^2 + \frac{I}{A} \left(\dot{\theta_k}^2 \right) \right] V_k \tag{4.9}$$

$$U = \sum_{k=1}^{\infty} \left[\frac{1}{2} \sum_{j=1}^{\infty} \frac{1}{2} [\tilde{\alpha}_{kj}(\kappa_{kj}) + \tilde{\alpha}_{jk}(\kappa_{jk})] V_j - \tilde{b}_k \theta_k \right] V_k$$

$$+ \sum_{k=1}^{\infty} \left[\frac{1}{2} \sum_{j=1}^{\infty} \frac{1}{2} [\hat{\alpha}_{kj}(\vartheta_{kj}) + \hat{\alpha}_{jk}(\vartheta_{jk})] V_j - \hat{b}_k u_k \right] V_k \tag{4.10}$$

Euler Lagrange equations can be expressed as

$$\frac{d}{dt} \frac{\partial L}{\partial \dot{u_k}} - \frac{\partial L}{\partial u_k} = 0 \tag{4.11}$$

$$\frac{d}{dt} \frac{\partial L}{\partial \dot{\theta_k}} - \frac{\partial L}{\partial \theta_k} = 0 \tag{4.12}$$

27

where

$$L = T - U \tag{4.13}$$

$$T = \cdots + \frac{1}{2}\rho \dot{u}_k{}^2 V_k + \frac{1}{2}\rho\frac{I}{A}\dot{\theta}_k{}^2 V_k + \cdots \tag{4.14}$$

$$-\frac{1}{2}\sum_{j=1}^{\infty}\left[\frac{1}{2}\left[\tilde{\alpha}_{kj}(\kappa_{kj}) + \tilde{\alpha}_{jk}(\kappa_{jk})\right]V_j\right]V_k\cdots$$

$$-\frac{1}{2}\sum_{j=1}^{\infty}\left[\frac{1}{2}[\hat{\alpha}_{kj}(\vartheta_{kj}) + \hat{\alpha}_{jk}(\vartheta_{jk})]V_j\right]V_k\cdots$$

$$-\frac{1}{2}\sum_{j=1}^{\infty}\left[\frac{1}{2}\left[\tilde{\alpha}_{kj}(\kappa_{kj}) + \tilde{\alpha}_{jk}(\kappa_{jk})\right]V_j\right]V_k\cdots$$

$$-\frac{1}{2}\sum_{j=1}^{\infty}\left[\frac{1}{2}[\hat{\alpha}_{kj}(\vartheta_{kj}) + \hat{\alpha}_{jk}(\vartheta_{jk})]V_j\right]V_k\cdots$$

$$+\tilde{b}_k\theta_k V_k + \hat{b}_k u_k V_k \tag{4.15}$$

$$L = \cdots + \frac{1}{2}\rho \dot{u}_k{}^2 V_k + \frac{1}{2}\rho\frac{I}{A}\dot{\theta}_k{}^2 V_k + \cdots$$

$$-\sum_{j=1}^{\infty}\left[\frac{1}{2}\left[\tilde{\alpha}_{kj}(\kappa_{kj}) + \tilde{\alpha}_{jk}(\kappa_{jk})\right]V_j\right]V_k\cdots$$

$$-\sum_{j=1}^{\infty}\left[\frac{1}{2}[\hat{\alpha}_{kj}(\vartheta_{kj}) + \hat{\alpha}_{jk}(\vartheta_{jk})]V_j\right]V_k\cdots$$

$$+\tilde{b}_k\theta_k V_k + \hat{b}_k u_k V_k \tag{4.16}$$

Putting this L in the Lagrange equation, we get

$$\rho\ddot{u}_k V_k + \sum_{j=1}^{\infty}\left[\frac{1}{2}\left[\frac{\partial\hat{\alpha}_{kj}(\vartheta_{kj})}{\partial\vartheta_{kj}}\frac{\partial\vartheta_{kj}}{\partial u_k} + \frac{\partial\hat{\alpha}_{jk}(\vartheta_{jk})}{\partial\vartheta_{jk}}\frac{\partial\vartheta_{jk}}{\partial u_k}\right]V_j\right]V_k - \hat{b}_k V_k = 0 \tag{4.17}$$

Let

$$\frac{1}{\xi_{jk}}\frac{\partial\hat{\alpha}_{kj}(\vartheta_{kj})}{\partial\vartheta_{kj}} = \hat{f}_{kj} \tag{4.18}$$

$$\frac{1}{\xi_{jk}}\frac{\partial\hat{\alpha}_{jk}(\vartheta_{jk})}{\partial\vartheta_{jk}} = \hat{f}_{jk} \tag{4.19}$$

28

Then we have

$$\rho \ddot{u}_k V_k + \sum_{j=1}^{\infty} \frac{1}{2} \left[\xi_{jk} \hat{f}_{kj} \frac{\partial \vartheta_{jk}}{\partial u_k} + \xi_{jk} \hat{f}_{jk} \frac{\partial \vartheta_{jk}}{\partial u_k} \right] V_j - \hat{b}_k = 0 \qquad (4.20)$$

Also

$$\rho \frac{I}{A} \ddot{\theta}_k + \sum_{j=1}^{\infty} \left[\frac{1}{2} \left[\frac{\partial \tilde{\alpha}_{kj}(\kappa_{kj})}{\partial \kappa_{kj}} \frac{\partial \kappa_{jk}}{\partial \theta_k} + \frac{\partial \tilde{\alpha}_{jk}(\kappa_{jk})}{\partial \kappa_{jk}} \frac{\partial \kappa_{jk}}{\partial \theta_k} \right] V_j \right] V_k$$

$$+ \sum_{j=1}^{\infty} \left[\frac{1}{2} \left[\frac{\partial \hat{\alpha}_{kj}(\vartheta_{kj})}{\partial \vartheta_{kj}} \frac{\partial \vartheta_{kj}}{\partial \theta_k} + \frac{\partial \hat{\alpha}_{jk}(\vartheta_{jk})}{\partial \vartheta_{jk}} \frac{\partial \vartheta_{jk}}{\partial \theta_k} \right] V_j \right] V_k - \tilde{b}_k V_k = 0 \qquad (4.21)$$

Let

$$\frac{1}{\xi_{jk}} \frac{\partial \tilde{\alpha}_{kj}(\kappa_{kj})}{\partial \kappa_{kj}} = \tilde{f}_{kj} \qquad (4.22)$$

$$\frac{1}{\xi_{jk}} \frac{\partial \tilde{\alpha}_{jk}(\kappa_{jk})}{\partial \kappa_{jk}} = \tilde{f}_{jk} \qquad (4.23)$$

Then we have

$$\rho \frac{I}{A} \ddot{\theta}_k + \sum_{j=1}^{\infty} \frac{1}{2} \xi_{jk} \left[\tilde{f}_{kj} \frac{\partial \kappa_{kj}}{\partial \theta_k} + \tilde{f}_{jk} \frac{\partial \kappa_{jk}}{\partial \theta_k} \right] V_j$$

$$+ \sum_{j=1}^{\infty} \frac{1}{2} \xi_{jk} \left[\hat{f}_{kj} \frac{\partial \vartheta_{kj}}{\partial \theta_k} + \hat{f}_{jk} \frac{\partial \vartheta_{jk}}{\partial \theta_k} \right] V_j - \tilde{b}_k = 0 \qquad (4.24)$$

where $\tilde{f}_{kj}, \tilde{f}_{jk} \hat{f}_{kj}, \hat{f}_{jk}$, are peridynamic interaction forces between material points j and k arising from bending and transverse shear deformation .

For linear behaviour, the interaction forces can also be defined as

$$\begin{aligned} \tilde{f}_{kj} &= c_b(\kappa_{kj}) & \tilde{f}_{jk} &= c_b(\kappa_{jk}) \\ \hat{f}_{kj} &= c_s(\vartheta_{kj}) & \hat{f}_{jk} &= c_s(\vartheta_{jk}) \end{aligned} \qquad (4.25)$$

The peridynamic parameter associated with bending and transverse shear deformation are c_s, c_b

Putting these values of peridynamic forces and corresponding shear angles and curvatures in EOM we have

$$\rho \ddot{u}_k = c_s \sum_{j=1}^{\infty} \left(\frac{u_j - u_k}{\xi_{jk}} - \frac{\theta_j + \theta_k}{2} sign(x_j - x_k) \right) V_j + \hat{b}_k \qquad (4.26)$$

$$\rho \frac{I}{A} \ddot{\theta}_k = c_b \sum_{j=1}^{\infty} \frac{\theta_j - \theta_k}{\xi_{jk}} V_j + \frac{1}{2} c_s \sum_{j=1}^{\infty} \left(\frac{u_j - u_k}{\xi_{jk}} - \frac{\theta_j + \theta_k}{2} sign(x_j - x_k) \right) V_j + \tilde{b}_k \qquad (4.27)$$

4.1.2   Validation with classical theory

Using Taylor series expansion we can express out of plane rotation and transverse shear deformation at material point j as

$$u_j = u_k + u_{k,x} \xi_{jk} sign(x_j - x_k) + \frac{1}{2} u_{k,xx} \xi_{jk}^2 \qquad (4.28)$$

$$\theta_j = \theta_k + \theta_{k,x} \xi_{jk} sign(x_j - x_k) + \frac{1}{2} \theta_{k,xx} \xi_{jk}^2 \qquad (4.29)$$

Putting these values in the EOM gives

$$\rho \ddot{u}_k = c_s \sum_{j=1}^{\infty} \left(\frac{u_k + u_{k,x} \xi_{jk} sign(x_j - x_k) + \frac{1}{2} u_{k,xx} \xi_{jk}^2 - u_k}{\xi_{jk}} \right)$$

$$-c_s \sum_{j=1}^{\infty} \left(\frac{\theta_k + \theta_{k,x} \xi_{jk} sign(x_j - x_k) + \frac{1}{2} \theta_{k,xx} \xi_{jk}^2 + \theta_k}{2} sign(x_j - x_k) \right) V_j + \hat{b}_k$$

$$= c_s \sum_{j=1}^{\infty} \left(0 + \frac{u_{k,xx} \xi_{jk}}{2} - \left(\theta_k sign(x_j - x_k) + \frac{\theta_{k,x} \xi_{jk}(1 - 0)}{2} + \frac{\theta_{k,xx}}{2} \xi_{jk}^2 sign(x_j - x_k) \right) \right) V_j + \hat{b}_k$$

$$= c_s \sum_{j=1}^{\infty} \left(\frac{u_{k,xx} \xi_{jk}}{2} - \frac{\theta_{k,x} \xi_{jk}}{2} \right) V_j + \hat{b}_k$$

$$\rho \ddot{u}_k = c_s \sum_{j=1}^{\infty} (u_{k,xx} - \theta_{k,x}) \xi_{jk} V_j + \hat{b}_k$$

$$(4.30)$$

Similarly

$$\rho \frac{I}{A} \ddot{\theta}_k = c_b \sum_{j=1}^{\infty} \theta_{k,xx} \xi_{jk} V_j + c_s \sum_{j=1}^{\infty} \left(u_{k,x} - \theta_k - \frac{1}{4} \theta_{k,xx} \xi_{jk}^2 \right) V_j + \tilde{b}_k \qquad (4.31)$$

Let $V_j = A\Delta\xi_{jk}$ where $\Delta\xi_{jk}$ is representing the spacing between two consecutive material points and replace summation by integration as $\Delta\xi_{jk}$ approaches zero. Now we have

$$\rho\ddot{u} = c_s \int_0^\delta (u_{,xx} - \theta_{,x})\xi A d\xi + \hat{b}$$

$$\rho\ddot{u} = c_s(u_{,xx} - \theta_{,x})A\frac{\delta^2}{2} + \hat{b} \tag{4.32}$$

Also

$$\rho\frac{I}{A}\ddot{\theta} = c_b \int_0^\delta \theta_{,xx}\xi A d\xi + c_s \int_0^\delta \left(u_{,x} - \theta - \frac{1}{4}\theta_{,xx}\xi^2\right)\xi A d\xi + \tilde{b}$$

$$= c_b\frac{\delta^2}{2}\theta_{,xx}A + \left(u_{,x}\frac{\delta^2}{2} - \theta\frac{\delta^2}{2} - \frac{\theta_{,xx}\delta^4}{16}\right)A + \tilde{b}$$

$$\rho\frac{I}{A}\ddot{\theta} = \frac{A\delta^2}{2}\left(c_b - c_s\frac{\delta^2}{8}\right)\theta_{,xx} + \frac{A\delta^2}{2}c_s(u_{,x} - \theta) + \tilde{b} \tag{4.33}$$

The above PD equations have same form as classical Timoschenko Beam equations

$$\rho\ddot{u} = kG(u_{,xx} + \theta_{,x}) + \hat{b}$$

$$\rho\frac{I}{A}\ddot{\theta} = \frac{EI}{A}\theta_{,xx} + kG(u_{,x} - \theta)\tilde{b} \tag{4.34}$$

Comparing coefficients we get the peridynamic material parameters as

$$c_s = \frac{2kG}{A\delta^2} \quad c_b = \frac{2EI}{\delta^2 A^2} + \frac{1}{4}\frac{kG}{A} \tag{4.35}$$

31

Chapter 5

APPLICATION TO MICROPOLAR BEAM

In micropolar continuum, it is assumed that there is a microstructre which can rotate independently from the surroundings. This means every particle contains six degrees of freedom , three translational motions which are assigned to macro element and three rotational ones which are assigned to the microstructure. In this method , in addition to force, particles apply moments to each other that is if a particle rotates, the other particles will apply moment to that particle to resist deformation.

At each particle of a micropolar continuum, it is assumed that there is a microstructure which can rotate independently from the surrounding medium.
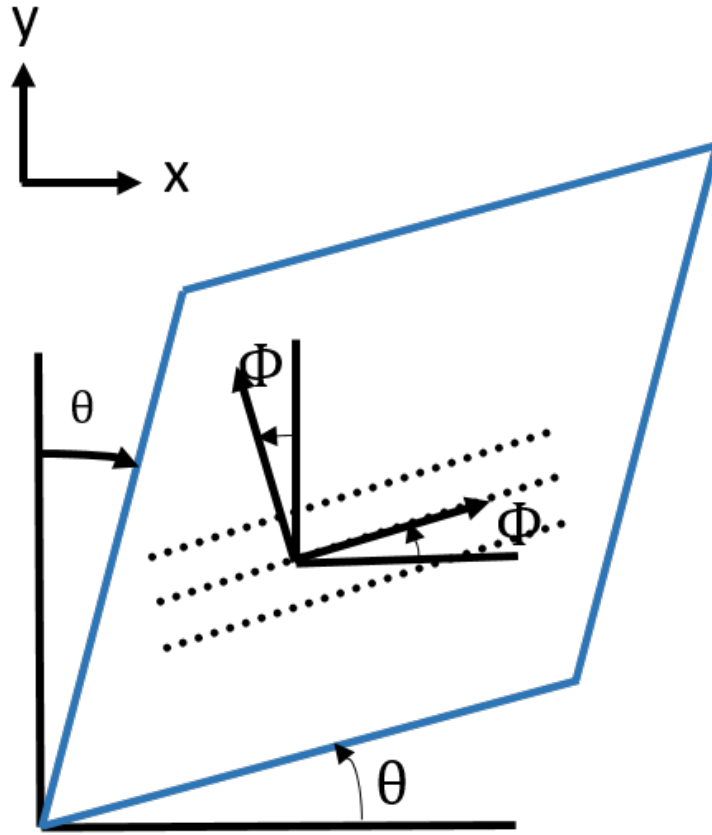
Figure 5.1: **Microrotation**

- Stress equilibrium

$$\frac{\partial \sigma_x}{\partial x} + \frac{\partial \tau_{yx}}{\partial y} = 0 \tag{5.1}$$

$$\frac{\partial \sigma_z}{\partial z} + \frac{\partial \tau_{xz}}{\partial x} = 0 \tag{5.2}$$

$$\frac{\partial m_{xy}}{\partial x} + \frac{\partial m_{zy}}{\partial y} + \tau_{xz} - \tau_{zx} = 0 \tag{5.3}$$
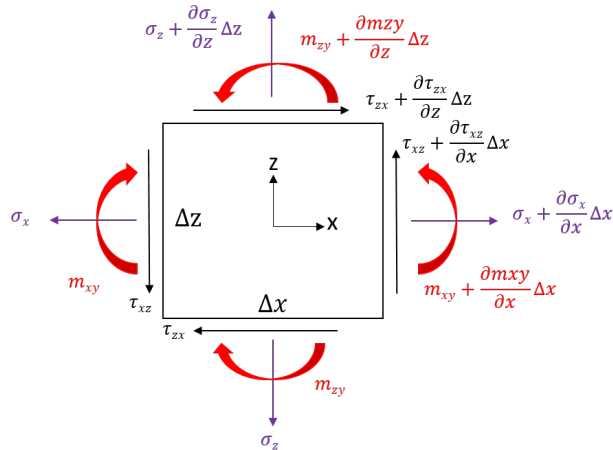
Figure 5.2: **Stresses acting on a planar micropolar solid.**

The shear stresses are not symmetric. The shear stresses are divided into antisymmetric and symmetric parts

$$\tau_s = \frac{\tau_{xz} + \tau_{zx}}{2} \tag{5.4}$$

$$\tau_a = \frac{\tau_{xz} - \tau_{zx}}{2} \tag{5.5}$$
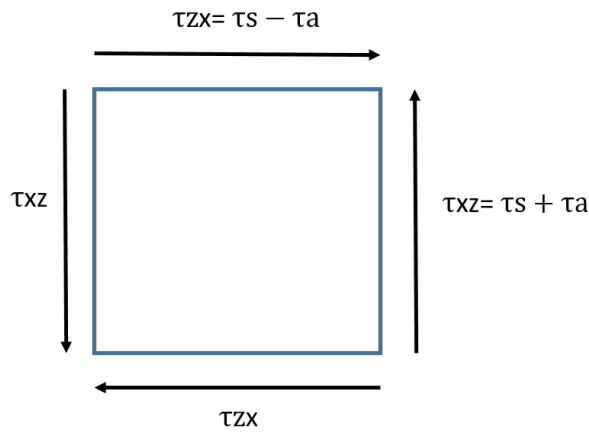
Figure 5.3: **Split of the shear stresses into symmetric and antisymmetric parts.**

The antisymmetric part is responsible for microrotation and symmetric part for usual shear deformation.

5.1 1D Micropolar PD Beam Theory

5.1.1 Geometry
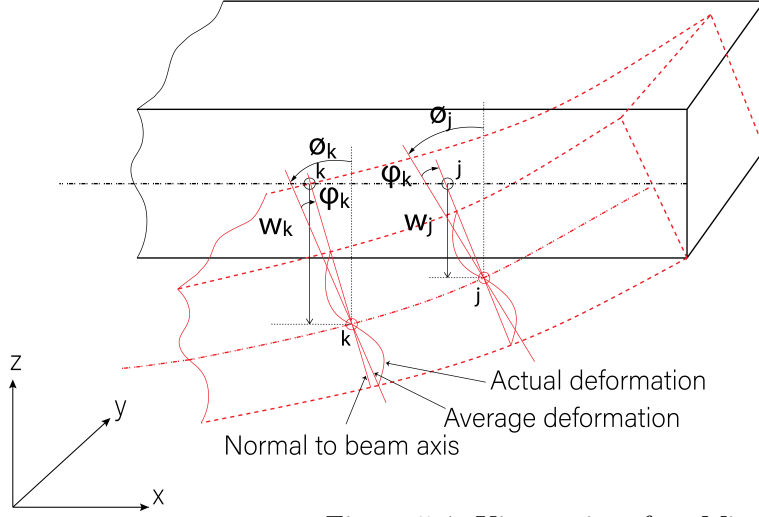
Figure 5.4: Kinematics of an Micropolar Beam .

5.1.2 General Equation of motion

$$m\ddot{u}(x,t) = \int_{x-\delta}^{x+\delta} (N_z[x] - N_z[x'])dx + B_z(x,t) \tag{5.6}$$

$$J\ddot{\phi}(x,t) = \int_{x-\delta}^{x+\delta} (\mu_y[x] - \mu_y[x'])dx$$

$$+ \frac{1}{2}\int_{x-\delta}^{x+\delta} (N_z[x] + N_z[x'])(x - x')dx$$

$$+ \frac{1}{2}\int_{x-\delta}^{x+\delta} (M_s[x] - M_s[x'])dx + L_y(x,t)$$

$$I\rho\ddot{\theta}(x,t) = \int_{x-\delta}^{x+\delta} (M[x] - M[x'])dx \tag{5.7}$$

$$- \frac{1}{2}\int_{x-\delta}^{x+\delta} (M_s[x] + M_s[x'])dx + L_z(x,t) \tag{5.8}$$

35

5.1.3   1D kinematic states

Relative transverse displacement $u[x] = u(x_j) - u(x_k)$

Relative macro-rotation $\theta[x] = \theta(x_j) - \theta(x_k)$

Relative micro-rotation $\phi[x] = \phi(x_j) - \phi(x_k)$

Average macro-rotation $\hat{\theta}[x] = \frac{1}{2}(\theta(x_j) + \theta(x_k))$

Average micro-rotation $\hat{\phi}[x] = \frac{1}{2}(\phi(x_j) + \phi(x_k))$

5.1.4   Constitutive relations

It is found out using the energy balance equations.

$$N_z(x_j - x_k) = A((\tilde{u} + \eta)\gamma_{\theta\phi} + \tilde{u}\gamma_{u\phi})(x_j - x_k)$$
$$\mu_y(x_j - x_k) = (A\beta\kappa_\phi)(x_j - x_k)$$
$$M(x_j - x_k) = (EI\kappa_\theta)(x_j - x_k)$$
$$M_s(x_j - x_k) = A((\tilde{u} + \eta)\gamma_{u\phi} + \tilde{u}\gamma_{\theta\phi})(x_j - x_k)^2$$

where $\gamma_{u\phi}$, κ_ϕ, κ_θ, $\gamma_{\theta\phi}$ are the non local strains which are given by:

$$\gamma_{u\phi} = \left[\sum_{j=1}^{N}((u_j - u_k) + \frac{1}{2}(\phi_j + \phi_k)(x_j - x_k))(x_j - x_k)LE\right]$$

$$\gamma_{\theta\phi} = \left[\sum_{j=1}^{N}(\frac{1}{2}(\phi_j + \phi_k) - \frac{1}{2}(\phi_j + \phi_k))(x_j - x_k)^2 LE\right]$$

$$\kappa_\phi = \left[\sum_{j=1}^{N}(\phi_j - \phi_k)(x_j - x_k)LE\right]$$

$$\kappa_\theta = \left[\sum_{j=1}^{N}(\theta_j - \theta_k)(x_j - x_k)LE\right]$$

5.1.5 Equation of motion

Putting the corresponding values in the equations $(33), (34), (35)$, we get EOM as

$$m\ddot{u}(x_k, t) = 2V(LE) \sum_{l=1}^{N} (\xi_{jk})((\tilde{\mu} + \eta) \sum_{j=1}^{N} \frac{1}{2}(\phi_j + \phi_k)(\xi_{jk})^2$$

$$+ \tilde{\mu} \sum_{j=1}^{N} (u_j - u_k)(\xi_{jk}) - \eta \sum_{j=1}^{N} \frac{1}{2}(\phi_j + \phi_k)(\xi_{jk})^2) \tag{5.9}$$

$$I\rho\ddot{\theta}(x_k, t) = \sum_{l=1}^{N} 2EI\xi_{jk}(LE)^2 \sum_{j=1}^{N} (\theta_j - \theta_k)(x_j - x_k)$$

$$- \frac{1}{2}(2V(LE) \sum_{l=1}^{N} (\xi_{jk})^2((\tilde{\mu} + \eta) \sum_{j=1}^{N} (u_j - u_k)(\xi_{jk})$$

$$+ \tilde{\mu} \sum_{j=1}^{N} \frac{1}{2}(\theta_j + \theta_k)(\xi_{jk})^2 + \eta \sum_{j=1}^{N} \frac{1}{2}(\phi_j + \phi_k)(\xi_{jk})^2) \tag{5.10}$$

$$J\ddot{\phi}(x_k, t) = 2VLE\beta \sum_{l=1}^{N} \xi_{jk} \sum_{j=1}^{N} (\phi_j - \phi_k)\xi_{jk}$$

$$- V(LE)\eta \sum_{l=1}^{N} (\xi_{jk})^2 (\sum_{j=1}^{N} \frac{1}{2}(\theta_j$$

$$+ \theta_k)(\xi_{jk})^2 + \sum_{j=1}^{N} (u_j - u_k)(\xi_{jk}))$$

$$+ 2V(LE)\eta \sum_{l=1}^{N} (\xi_{jk})^2 \sum_{j=1}^{N} \frac{1}{2}(\phi_j + \phi_k)(\xi_{jk})^2 \tag{5.11}$$

- By neglecting the microrotation and putting micropolar constant η as zero , we get the EOM for Timoshenko beam by adjusting the constants as

$$\rho\ddot{u}_k = c_s \sum_{j=1}^{\infty} \left(\frac{u_j - u_k}{\xi_{jk}} - \frac{\theta_j + \theta_k}{2} sgn(x_j - x_k) \right) V_j + \hat{b}_k \tag{5.12}$$

$$\rho \frac{I}{A} \ddot{\theta}_k =$$

$$c_b \sum_{j=1}^{\infty} \frac{\theta_j - \theta_k}{\xi_{jk}} V_j + \frac{1}{2} c_s \sum_{j=1}^{\infty} \left(\frac{u_j - u_k}{\xi_{jk}} sgn(x_j - x_k) - \frac{\theta_j + \theta_k}{2} \right) \xi_{jk} V_j + \tilde{b}_k \qquad (5.13)$$

- Further neglecting the shear deformation and adjusting the constants, we get EOM for Euler Bernoulli beam as

$$\rho_k \ddot{u}_k = ad^2 \sum_{j=1}^{\infty} \frac{1}{\xi_{jk}^2} \left(\sum_{i^k=1}^{\infty} \frac{u_{i^k} - u_k}{\xi_{i^k k}^2} V_{i^k} - \sum_{i^j=1}^{\infty} \frac{u_{i^j} - u_j}{\xi_{i^j j}^2} V_{i^j} \right) V_j + \hat{b}_k \qquad (5.14)$$

Chapter 6

PROBLEM STATEMENT

6.1   Problem

- A simply supported beam

- Length of beam(L) = 1m

- Area of cross section(A)= $0.01 \times 0.01 m^2$

- Young's modulus(E)= 200GPa

- Point load at centre(P) = 50N

- Horizon size(δ) = 2× length of an elemnt
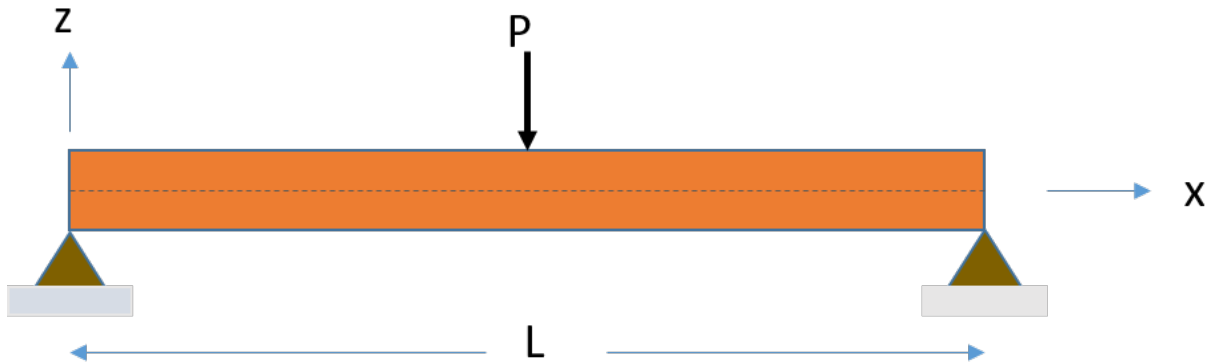
Figure 6.1: **SSB with load of 50 kN**

6.1.1 Solution

- Discretize the beam into single row of N no. of material points.

- Distance between material points is $LE = 1/N$

- Two fictitious volumes are created on left hand and right hand of the beam with length equal to horizon size .
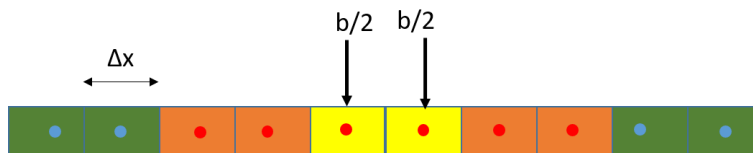
Figure 6.2: **Discretization of a Beam**

- If there are odd no. of elements, then loading is applied to middle material point with body force $b = \frac{P}{A*LE}$

- If there are even no. of elements, then loading is applied to two middle material points with body force $b = \frac{P}{2*A*LE}$ on each of the two material point.

- .Boundary condition is applied by extending the deformed shape of the beam in the fictitious volumes as shown
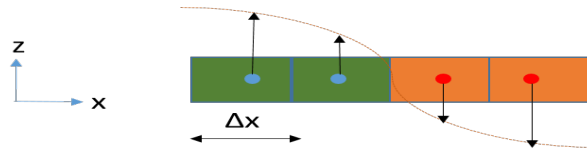
Figure 6.3: **Negative Mirror image of Displacements**

- Similarly it is done for other support also.The displacements of the material points in the fictitious volume are specified as

$$u_1 = -u_4$$
$$u_2 = -u_3$$
$$u_{99} = -u_{98}$$
$$u_{100} = -u_{97}$$

- Equation (3.18) is written in matrix form as

$$[K]\{U\} = \{B\} \tag{6.1}$$

where $\{U\}, [K]$ and $\{B\}$ represents the displacement matrix,stiffness matrix and body force matrix respectively.

- Lets displacement matrix be expressed as

$$\{U\} = [R]\{\hat{U}\} \tag{6.2}$$

where$[R]$ represents matrix used to transform displacement matrix into reduced displacement matrix i.e $\{\hat{U}\}$.
The reduced displacement matrix contain displacements of material points which are in the beam only.

41

- Imposing boundary conditions, we have

$$R = \begin{bmatrix} 0 & -1 & 0 & . & . & . & . \\ -1 & 0 & 0 & . & . & . & . \\ 1 & 0 & 0 & . & . & . & . \\ 0 & 1 & 0 & . & . & . & . \\ . & . & . & . & . & . & . \\ . & . & . & . & . & . & . \\ . & . & . & . & 0 & 0 & 1 \\ . & . & . & . & 0 & 0 & -1 \\ . & . & . & . & 0 & -1 & 0 \end{bmatrix}_{N \times (N-2\delta)}$$

$$\hat{U} = \begin{bmatrix} u_3 \\ u_4 \\ . \\ . \\ . \\ . \\ u_{97} \\ u_{98} \end{bmatrix}_{(N-2\delta) \times 1}$$

- Putting stiffness , transformation,reduced displacement and body force matrix in the following equation we will get the unknown displacements

$$[R]^T[K][R]\{\hat{U}\} = [R]^T\{B\} \tag{6.3}$$

42

Chapter 7

RESULTS AND DISCUSSIONS

7.1 Euler Bernoulli Beam

7.1.1 Simply Supported Beam
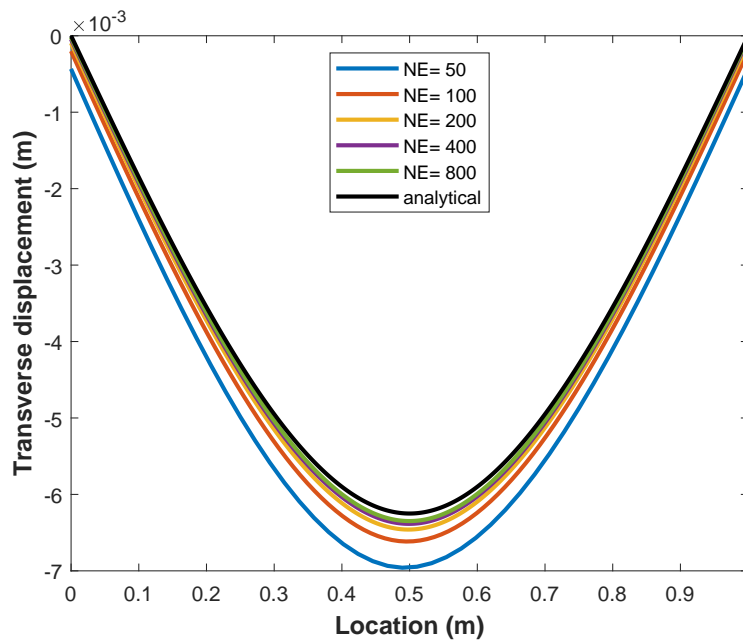
Figure 7.1: **Plot with varying no. of elements and constant horizon of 2*LE (EB Beam)**

- Analytical solution

$$Deflection = \frac{P * X}{48 * E * I}(3L^2 - 4X^2) \quad X < L/2$$

- This is the plot between transverse displacements of the material points and their coordinates .

- The maximum deflection is at centre of the beam and is equal to 6.25 mm analytically.

- As the no. of elements are increasing from NE=50 to NE=800, the graph is converging.

- After NE=100, it seems graphs overlaps a little to each other for NE=200,400,800.

- For NE=800, the graph is totally compatible with the analytical solution.
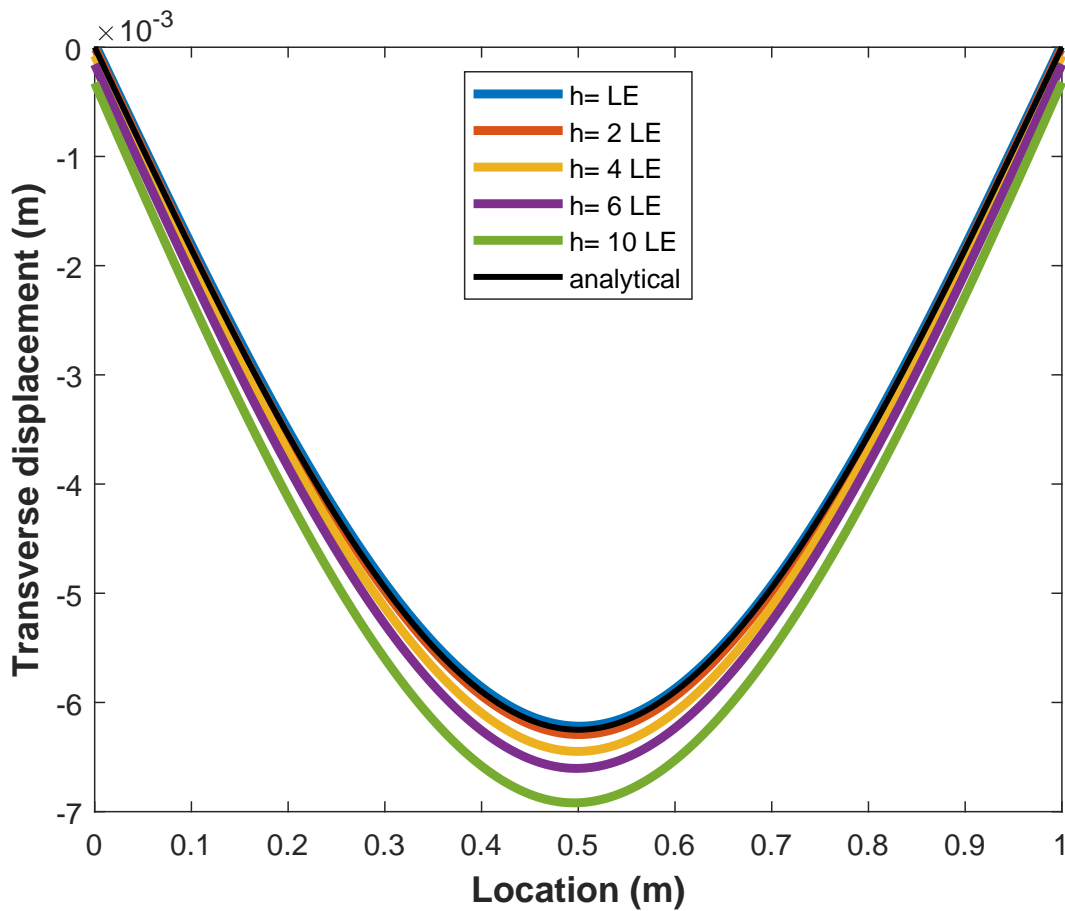
Figure 7.2: **Plot with varying horizon length and constant no. of elements equal to 500 (EB Beam)**

- This is the plot beyween transverse displacements of the material points and their coordinates .

- The maximum deflection is at centre of the beam and is equal to 6.25 mm analytically.

- As the horizon size is increasing from h=LE to h=10 LE, the graph is diverging

- After h=2LE, graph discourages itself to overlap from h=4 LE, 6 LE, 8 LE.

- For h=2 LE the graph is totally compatible with the analytical solution.

7.1.2 Cantilever Beam

- Length of beam(L) = 1m

- Area of cross section(A)= $0.01 \times 0.01 m^2$

- Young's modulus(E)= 200GPa

- Point load at free end(P) = 50N

- Horizon size(δ) = 2× length of an elemnt
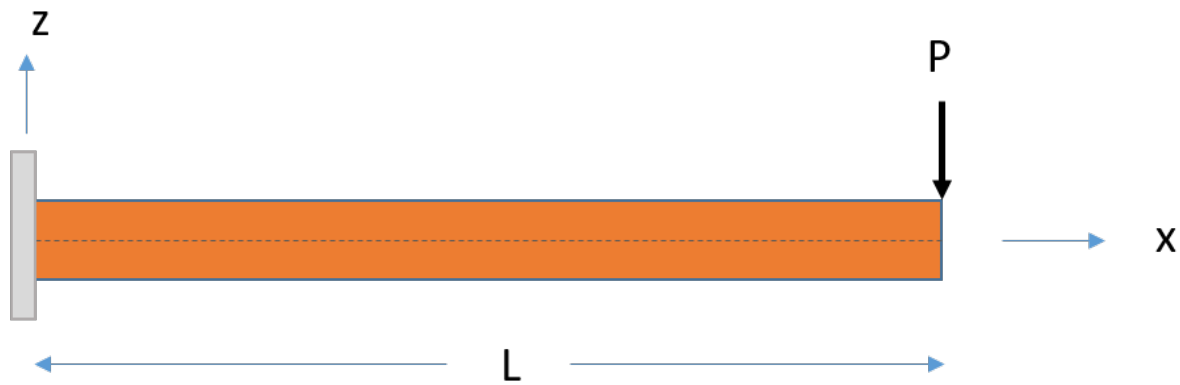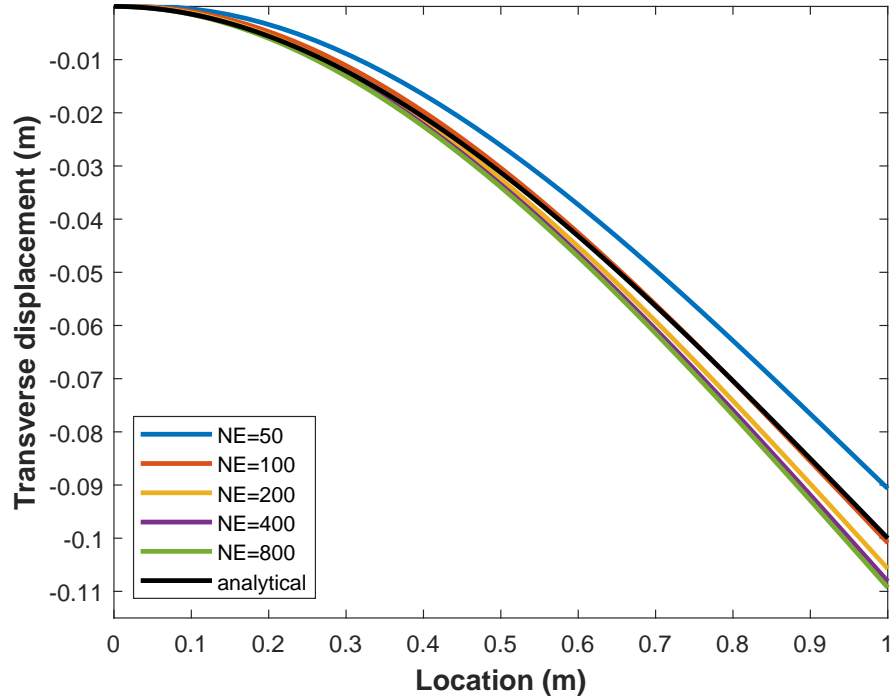

Figure 7.3: **Cantilever Beam with load 50 kN**

Figure 7.4: **Plot with varying no. of elements and constant horizon of 2*LE (EB Beam)**

- Analytical solution

$$DEflection = \frac{P*(L-X)^3}{3*E*I}$$

(7.1)

- This is the plot between transverse displacements of the material points and their coordinates .

- The maximum deflection is at free end of the beam and is equal to 100 mm analytically.

- As the no. of elements are increasing from NE=50 to NE=800, the graph is converging.

- But the correct overlapping of analytical solution is with the graph with NE= 100.

- For NE=50 , the displacements in peridynamics are coming greater than the analytical solutions.

Figure 7.5: **Plot with varying horizon size and constant no. of elements equal to 500 (EB Beam)**
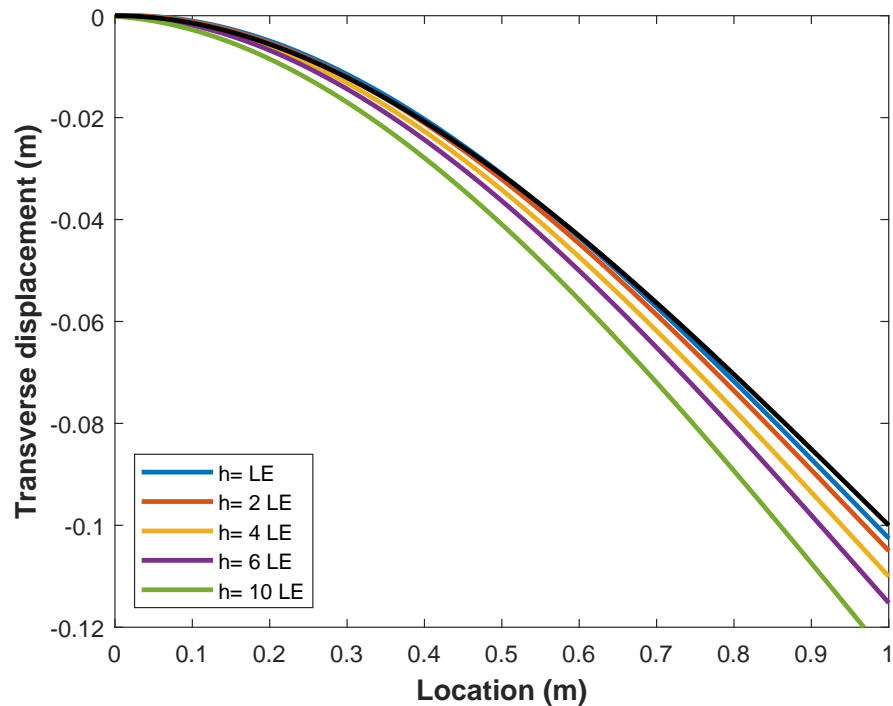
- This is the plot beyween transverse displacements of the material points and their coordinates .

- The maximum deflection is at the free end of the beam and is equal to 100 mm analytically.

- As the horizon size is increasing from h=LE to h=10 LE, the graph is diverging

- After h=2LE, graph discourages itself to overlap from h=4 LE, 6 LE, 8 LE.

- For h= LE the graph is totally compatible with the analytical solution.

7.1.3 Clamped Clamped Beam

- Length of beam(L) = 1m

- Area of cross section(A)= $0.01 \times 0.01m^2$

- Young's modulus(E)= 200GPa

- Point load at centre(P) = 50N

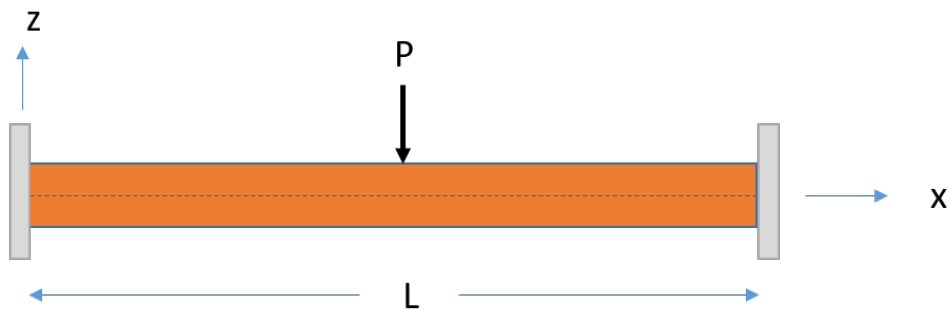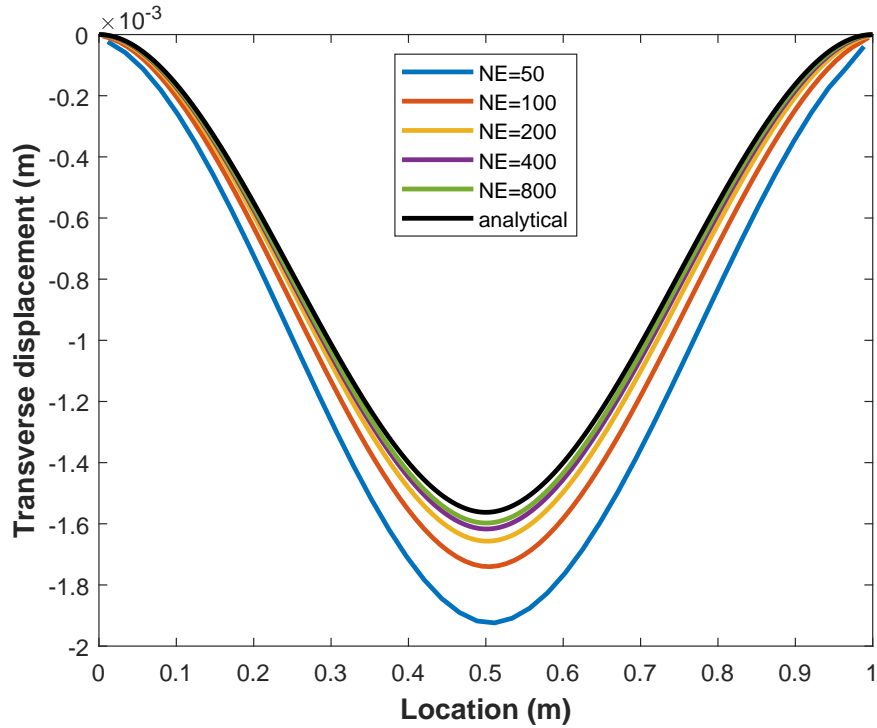- Horizon size(δ) = 2$\times$ length of an elemnt

Figure 7.6: **CCB with load 50 kN**

Figure 7.7: **Plot with varying no. of elements and constant horizon of 2*LE (EB Beam)**

- Analytical solution

$$Deflection = \frac{P * X}{48 * E * I}(3L - 4X) \quad X < L/2$$

- This is the plot between transverse displacements of the material points and their coordinates .

- The maximum deflection is at centre of the beam and is equal to 1.6 mm analytically.

- As the no. of elements are increasing from NE=50 to NE=800, the graph is converging.

- After NE=100, it seems graphs overlaps a little to each other for NE=200,400,800.

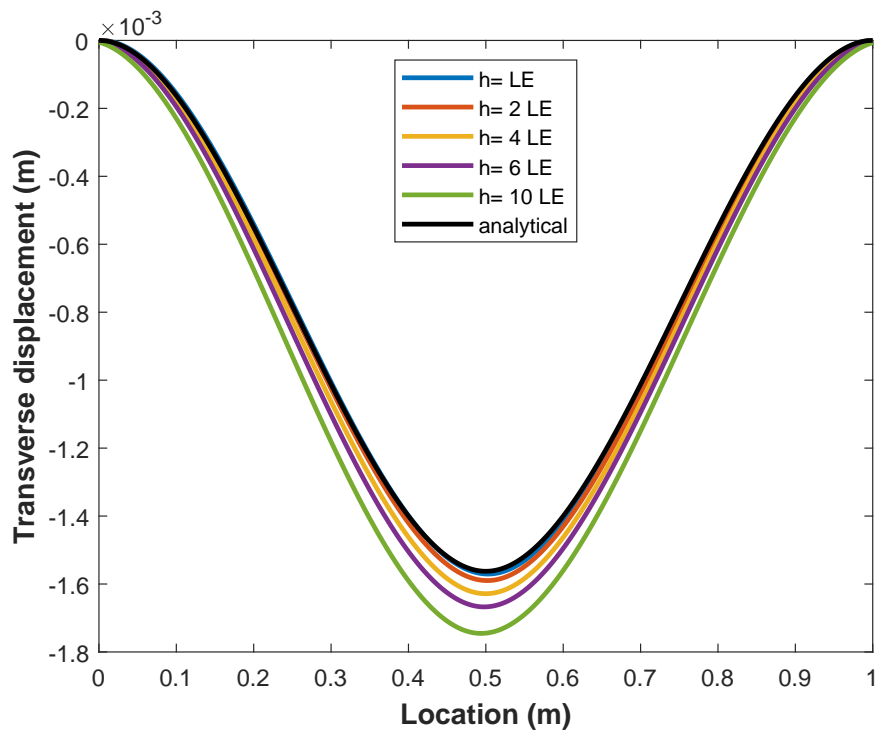- For NE=800, the graph is totally compatible with the analytical solution.

Figure 7.8: **Plot with varying horizon length and constant no. of elements equal to 500 (EB Beam)**

- This is the plot beyween transverse displacements of the material points and their coordinates .

- The maximum deflection is at centre of the beam and is equal to 1.6 mm analytically.

- As the horizon size is increasing from h=LE to h=10 LE, the graph is diverging

- After h=2LE, graph discourages itself to overlap from h=4 LE, 6 LE, 8 LE.

- For h= LE the graph is totally compatible with the analytical solution.

7.2   Timoshenko Beam

7.2.1   Simply Supported Beam

- Length of beam = 1m

- Area of cross section = $0.1 \times 0.1m^2$

- Young's modulus = 200GPa
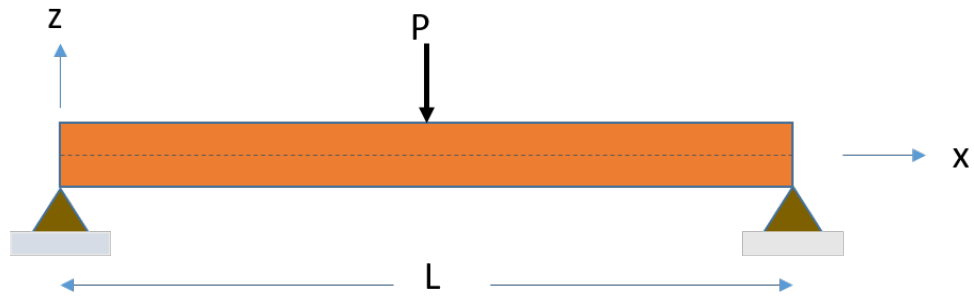
- Point load at centre = 500kN

Figure 7.9: **SSB with load 500 kN**

- Analytical solution

$$Deflection = \frac{P * X}{48 * E * I}(3L^2 - 4X^2) \quad X < L/2$$

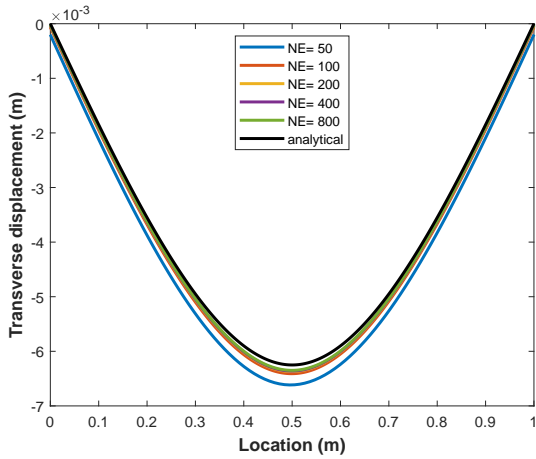$$Rotation = \frac{P}{16 * E * I}(L^2 - 4X^2) \quad X < L/2$$

Figure 7.10: **Plot between transverse displacement and length of beam (Timoshenko Beam)**
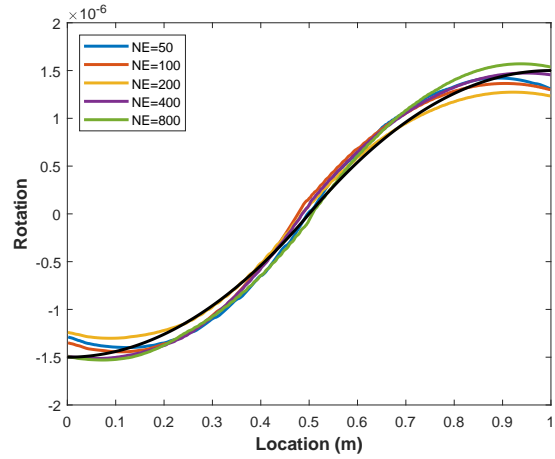

Figure 7.11: **Plot between rotation and length of beam (Timoshenko Beam)**

- These are the plots between transverse displacement,and rotation of material points and their coordinates.

- The maximum displacement is at centre and is equal to 6.25 mm .The maximum rotation is at supports and is equal to 1.5×10^{-6} and is equal to zero at mid point of the beam analytically.

- For the transverse displacement, as the no. of elements are increasing from NE=50 to NE=800, graph is converging.

- For the rotation the graph is somewhat not uniform , the graph for NE=800 overlaps with analytical one at starting, then from X=0.2m to X=0.7m , NE=200 overlaps with analytical one, then in the end NE=400 overlaps with analytical one.

- For transverse displacement, from NE=100, the begins to overlap each other and it fully complies with the analytical solution.

53

7.2.2 Cantilever Beam

- Length of beam = 1m

- Area of cross section = $0.1 \times 0.1 m^2$
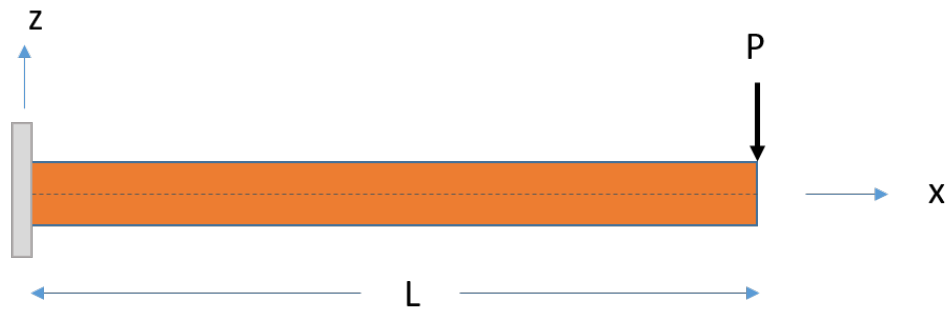
- Young's modulus = 200GPa

- Point load at centre = 500kN

Figure 7.12: **Cantilever Beam with load 500 kN**

- Analytical solution

$$Deflection = \frac{P * (L - X)^3}{3 * E * I}$$
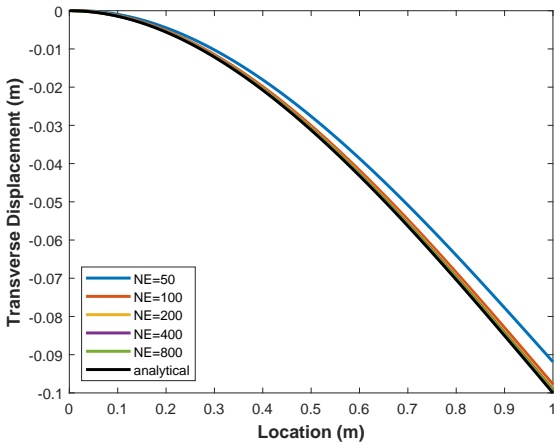$$Rotation = \frac{P * (L - X)^2}{2 * E * I}$$

Figure 7.13: **Plot between transverse displacement and length of beam (Timoshenko Beam)**
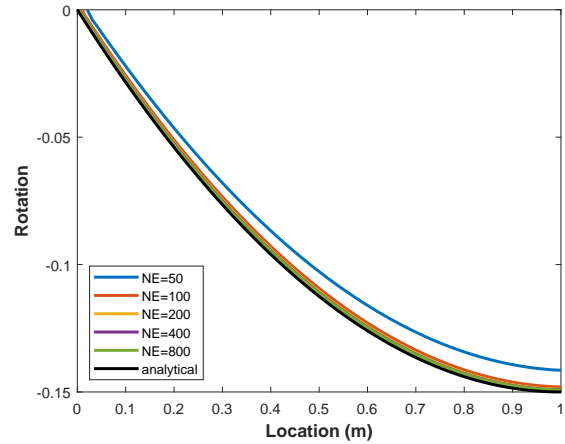

Figure 7.14: **Plot between rotation and length of beam (Timoshenko Beam)**

- These are the plots between transverse displacement,and rotation of material points and their coordinates.

- The maximum displacement is at free end and is equal to 100 mm .The maximum rotation is at free end and is equal to 0.15 rad.

- For the transverse displacement, as the no. of elements are increasing from NE=50 to NE=800, graph is converging

- For the rotation also , as the no. of elements are increasing from NE=50 to NE=800, graph is converging

- For transverse displacement, from NE=100, the graph begins to overlap each other and it fully complies with the analytical solution, only for NE=50 graph seems to be having less displacement values

- For rotation also, from NE=100, the graph begins to overlap each other and it fully complies with the analytical solution, only for NE=50 graph seems to be having less rotation values

7.2.3 Clamped Clamped Beam

- Length of beam = 1m

- Area of cross section = $0.1 \times 0.1 m^2$

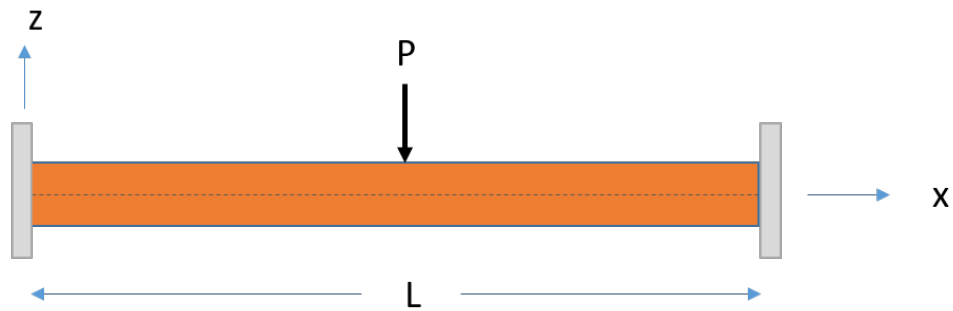- Young's modulus = 200GPa

- Point load at centre = 500kN

Figure 7.15: **CCB with load 500 kN**

- Analytical solution

$$Deflection = \frac{P*X}{48*E*I}(3L - 4X) \quad X < L/2$$
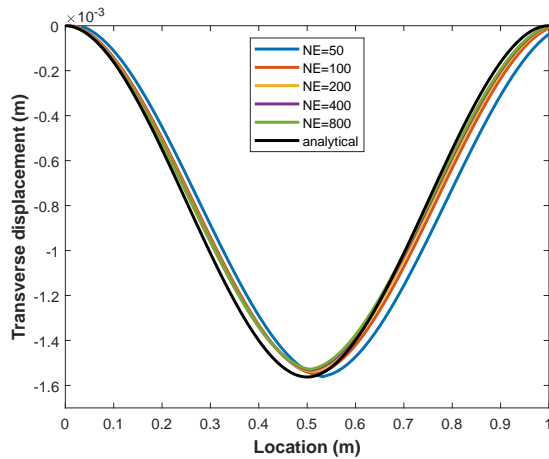$$Rotation = \frac{P*X}{8*E*I}(L - 2X) \quad X < L/2$$

Figure 7.16: **Plot between transverse displacement and length of beam (Timoshenko Beam)**
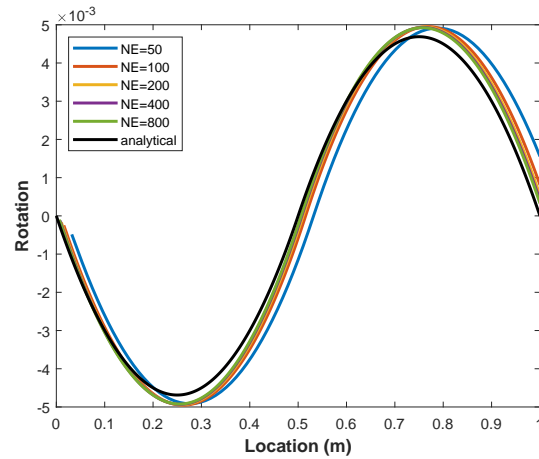

Figure 7.17: **Plot between rotation and length of beam (Timoshenko Beam)**

- These are the plots between transverse displacement,and rotation of material points and their coordinates.

- The maximum displacement is at centre and is equal to 1.6 mm .The maximum rotation is at a distance of 0.25 m from each supports and is equal to 4.5×10^{-3} and is equal to zero at each support and middle of the beam.

- For the transverse displacement, upto a distance of 0.5 m, all graphs seems to be overlapping but after 0.5 m , the graph with NE=50 begins to diverge.For NE =50, the maximum value of deflection comes as X=0.55 m.

- For the rotation all the graphs seems to be ovelapping but showing a greater value of maximum rotation . Upto X=0.2 m , from X=0.4 m to 0.7m and near the support, the graph with NE=800 fully complies with tha analytical solution.

57

Chapter 8

SCOPE OF PRESENT WORK

- PRODUCTION SOFTWARE
  * Unify Peridigm/Sierra/EMU
  * Address usability and interface issues
  * Material model library
- SOLVERS AND NUMERICAL METHODS
  * SPH, kernel methods connection
  * Next gen platforms
  * Eulerian and ALE capability
- MATERIAL/DAMAGE MODELING
  * Ductile failure
  * continuum damage mechanics
  * Quasistatic material failure
  * Digital Image correlation (DIC)
  * Nonlocal deformation measures
- MULTISCALE
  * Scalable multiscale methods
  * Coarse graining
  * Atomistic-to-continuum coupling
  * General tool for material failure
- MATH AND THEORY

- * Quantify uncertainty specially in fracture
- * Contact algorithms
- * Material stability

- – MULTIPHYSICS
  - * Math and numeric for multiphysics
  - * Geological applications
  - * Fluid-structure interaction
  - * Diffusion, chemical reactions
  - * Electromagnetic fields
  - * Electronics and MEMS reliability
  - * Friction

Bibliography

[1] Francesco dell'Isola, Ugo Andreaus, and Luca Placidi. *A still topical contribution of Gabrio Piola to Continuum Mechanics: the creation of peridynamics, nonlocal and higher gradient continuum mechanics.* 2014.

[2] Ning Liu and Dahsin Liu. Peridynamic modeling of impact damage in 3 point bending beam with offset notch. *Applied Mathematics and Mechanics*, 38:99–110, 2017.

[3] A Freimanis and A Paegltis. Modal analysis of isotropic beams in peridynamics. *IOP Conference Series: Materials Science and Engineering*, 251:1–7, 2017.

[4] B.O Chen, Ning Liu, and Guolai Yang. Application of peridynamics in predicting beam vibration and impact damage. *Journal of Vibro Enineering*, 21:2369–2378, 2015.

[5] James O' Gardy and John Foster. Peridynamic beams: A non-ordinary, state-based model. *International Journal of Solids and Structures*, 51:3177–3183, 2014.

[6] S A Silling. Reformulation of elasticity theory for discontinuities and long range forces. *Journal of Mechanics and Physics of Solids*, 48:175–209, 2000.

[7] J F Kalthoff and S Winkler. Failure mode transition at high rates of shear loading. *Impact Loading and Dynamic Behaviour of Materials*, 1:185–195, 1988.

[8] S . A. Siling and E. Askari. A meshfree method based on the peridynamic model of solid mechanics. *Computers and Structures*, 83:1526–1535, 2004.

[9] James O' Gardy and John Foster. Peridynamic plates and flat shells:a non ordinary state based model. *International Journal of Solids and Structures*, 51:4572–4579, 2014.

[10] A Shafei. Dynamic crack propagation in plates weakened by inclined cracks :investigation based on periynamics. *Frontiers of structural and civil engineering*, 12, 2018.

[11] C Diyaroglu, E Oterkus, E Madenci, T Rabczuk, and A Siddiq. Peridynamic modeling of composites laminates under explosion. *Composite Structures*, 144, 2016.

[12] Yile Hu, Erdogan Madenci, and Nam Phan. Peridynamic modeling of defects in composites. *Structural Dynamics and Materials Conference*, 2015.

[13] Jifeng Xu, Abe Askari, Olaf Wreckner, and Stewart Silling. Peridynmic analysis of impact damage in composite laminates. *Journal of Aerospace Engineering*, 21:23–42, 2008.

[14] Wenke Hu, Youn Doh Ha, and Florin Babaru. Modeling dynamic fracture and damage in a fiber reinforced composite lamina with peridynamics. *Journal for Multiscale Computational Engineering,*, 9:707–726, 2011.

[15] Yozo Mikata. Analytical solution of peristatic and peridynamics problems for a 1D infinite rod. *International Journal of Solids and Structures*, 49:2887–2897, 2012.

[16] G. Sarego, Q. V. Le, F. Bobaru, M. Zaccariotto, and U. Galvanetto. Linearized state based peridynamics for 2D problems. *International Journal for Numerical methods in Engineering*, 108:1174–1197, 2016.

[17] Q.V. Le, W.K. Chan, and J. Schwartz. A 2D ordinary state based peridynamic model for linearly elastic solids. *International journal for numeriacal methods in engineering*, 98(4):547–561, 2014.

[18] A.Tastan, U.Yoluma, M.A.Güleran M.Zaccariotto, and U.Galvanetto. A 2D peridynamic model for failure analysis of orthotropic thin plates due to bending. *Procedia Structural Integrity*, 2:261–268, 2016.

[19] Michael Taylor and David J Steigmann. A 2 D peridynamic model for thin plates. *Mathematics and Mechanics of solids*, 2013.